

CLARUS - ZEISS EXPERIENCE

Ultra-Widefield True Color Fundus Imaging



Centro di eccellenza Zeiss per la diagnostica

www.amedeolucente.it



ZEISS

Reflex free
RETINAL CAMERA after
NORDENSON

AN instrument of simple construction which can be used in any hospital or private office without special training in photographic technique. To obtain a satisfactory record of fundus condition is a matter of minutes only.

Price \$768 f.o.b. N.Y.

CARL ZEISS, Inc., 485 Fifth Ave., New York
Pacific Coast Branch: 728 South Hill Street, Los Angeles, Calif.

**Zeiss Reflex free Retinal Camera
after Nordenson 1930**

Price \$ 768 f.o.b. N.Y. (free of board)

768 \$ x 19,91 \$ = 15.290 \$

1 \$ 1933 ~ 19,91 \$ today

1\$ 1933 = 10 bottles of beer

Ford Model T ~ 850 \$ 1911; ~ 300 \$ 1927

Paga Operaio della Ford 5-8 \$/giorno

by: <https://scenarieconomici.it>

La prima fundus camera era basata sull'ottica geometrica secondo i principi dell'oculista svedese **Allvar Gullstrand (1862-1930), premio Nobel per la Medicina nel 1911**

Progetto di J.W. Nordenson del 1925 (1883-1965)

Realizzata da Carl Zeiss nel 1926

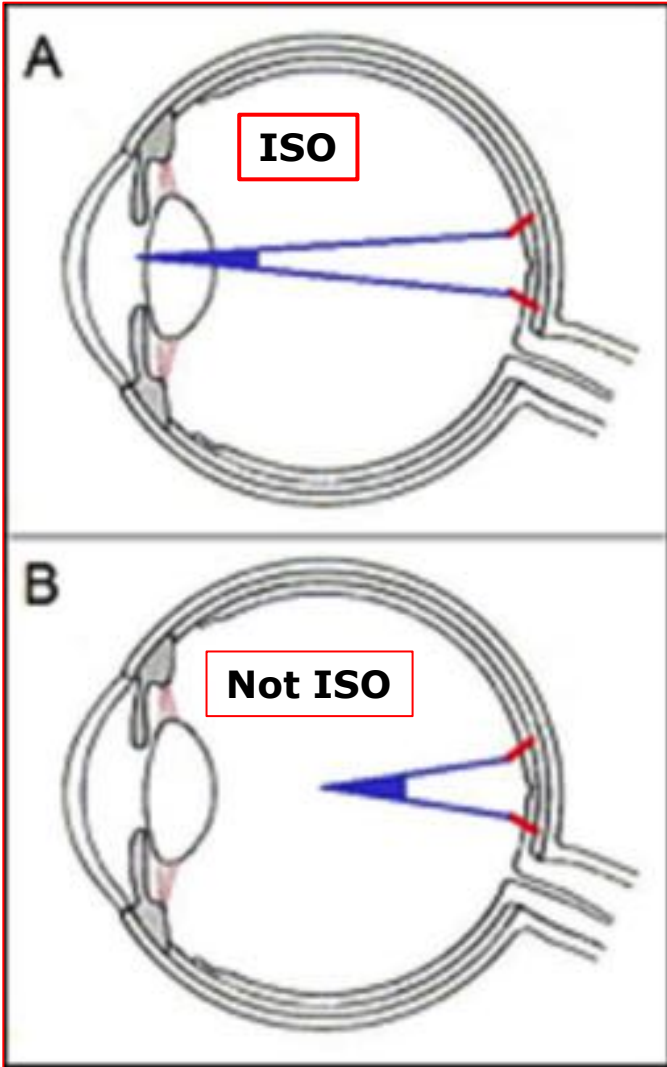
Commercializzata nel 1930

Apertura angolare di 10°, subito dopo di 20°

0,5 secondi esposizione, color film come pellicola

Dopo lunga elaborazione si passa a 30°, standard nella retinografia fino alla pubblicazione dell'ETDRS

**Switch-off retinal imaging 45°/60° v/s WF & UWF
Clarus 500 Zeiss: Italia **aprile 2018****



FoV Field of View
WF Widefield Imaging $FoV \geq 50^\circ$
UWF Ultra Widefield Imaging $FoV \geq 100^\circ$

ISO 10940 International Organization for Standardization
Centro dell'apertura angolare nell'area pupillare

90° ISO~ 133° not ISO

133° ISO~ 200° not ISO

WF & UWF



Ophthalmic Services Guidance Ophthalmic Imaging March 2021

Widefield imaging WF are considered to be “**single**” images depicting retinal anatomy **beyond the posterior pole, but posterior to the vortex vein ampulla in all 4 quadrants**

Ultra-Widefield UWF images depicting retinal anatomy **beyond the vortex vein ampulla**

Choudhry, N.; Duker, J.S.; Freund, K.B.; Kiss, S.; Querques, G.; Rosen, R.; Sarraf, D.; Souied, E.H.; Stanga, P.E.; Staurenghi, G.; et al. Classification and Guidelines for Widefield Imaging: Recommendations from the International Widefield Imaging Study Group. **Ophthalmol. Retin.** 2019, 3, 843–849.

Ultra-widefield imaging UWF as images showing retinal anatomic features **anterior to the vortex vein ampullae in all four quadrants.**

Mohamed Ashraf, Jerry D. Cavallerano, Jennifer K. Sun, Paolo S. Silva and Lloyd Paul Aiello.
Ultrawide Field Imaging in Diabetic Retinopathy: Exploring the Role of Quantitative Metrics.
J. Clin. Med. 2021, 10, 3300

- It is important to note that at present, both **Wide and Ultra-Wide Field** adjective descriptions **can be applied not only to colour, pseudo-colour and fundus autofluorescence but also to OCT cross-sectional, topographic and angiographic imaging**, all OCT imaging **with and without 3-D rendering** (The Royal College of ophthalmologists London)
- **UWF imaging allows** the visualization of a substantially **greater area of the retina compared to the standard seven field Early Treatment Diabetic Retinopathy Study (ETDRS) fields (82% vs. 30%)**
- **UWF allows** the identification of **DR lesions predominantly outside the ETDRS seven-standard fields**, referred to as **predominantly peripheral lesions (PPL)**
- Several studies have demonstrated that **PPL are present in 30–40% of eyes with DR**
- **PPL suggested** a more severe DR level in **11% of eyes**
- **PPL have been associated with a 3.2 fold increased risk DR progression** and a **4.7 fold increased risk for progression to proliferative DR over four years**



The diagram shows a fundus image with several overlapping circular fields of view. A central field is labeled 'Direct Ophthalmoscope 10-15°'. A larger field is labeled 'Slit Lamp with 90 diopter lens'. A very large field is labeled 'ZEISS CLARUS Ultra-widefield'. A box on the left contains the text 'ETDRS 7 campi 75°'. Other labels include 'Indirect Ophthalmoscope with 20 diopter lens - 37°' and 'Traditional Fundus - 45°'. The ZEISS CLARUS Widefield is also labeled.

ETDRS 7 campi 75°

ZEISS CLARUS Widefield
Covers ETDRS 7 standard fields

Traditional Fundus - 45°

Indirect Ophthalmoscope with 20 diopter lens - 37°

Slit Lamp with 90 diopter lens

Direct Ophthalmoscope 10-15°

ZEISS CLARUS Ultra-widefield

Early Treatment Diabetic Retinopathy Study

Studio clinico multicentrico sostenuto dal NEI National Eye Institute

Question: efficacia fotocoagulazione argon laser v/s aspirina in NPDR Non-Proliferative Diabetic Retinopathy / HR-PDR High-Risk Proliferative Diabetic Retinopathy

Strat: 1979

End: 1985

Follow-up: 1988

Published: 1991

22 centri

3.711 pazienti 18 →70 aa ♀♂

period 4 years

not laser treatment

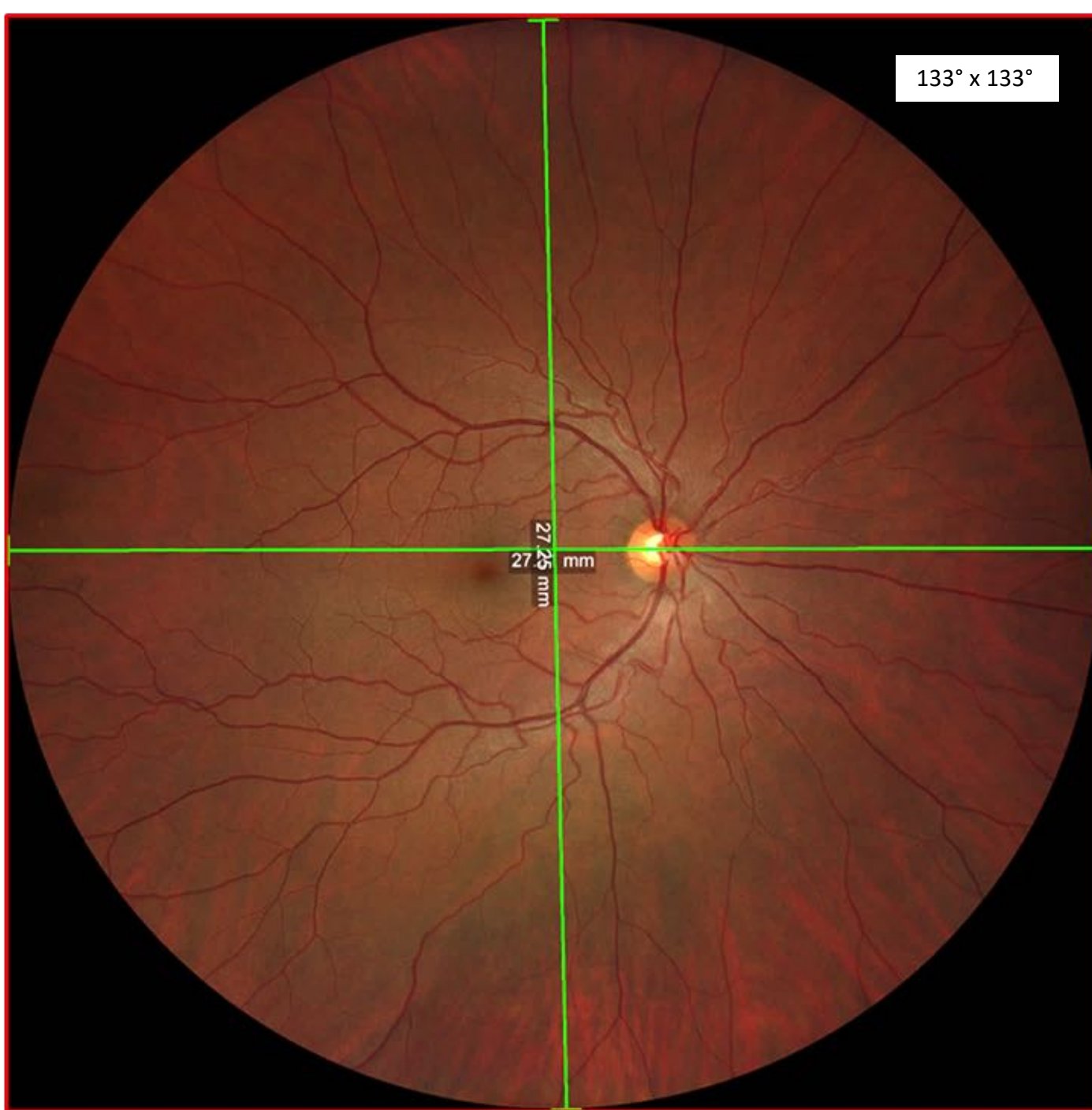
visus ≥ 20/40

Imaging 7 campi oltre le arcate vascolari





? 82%
? 267°



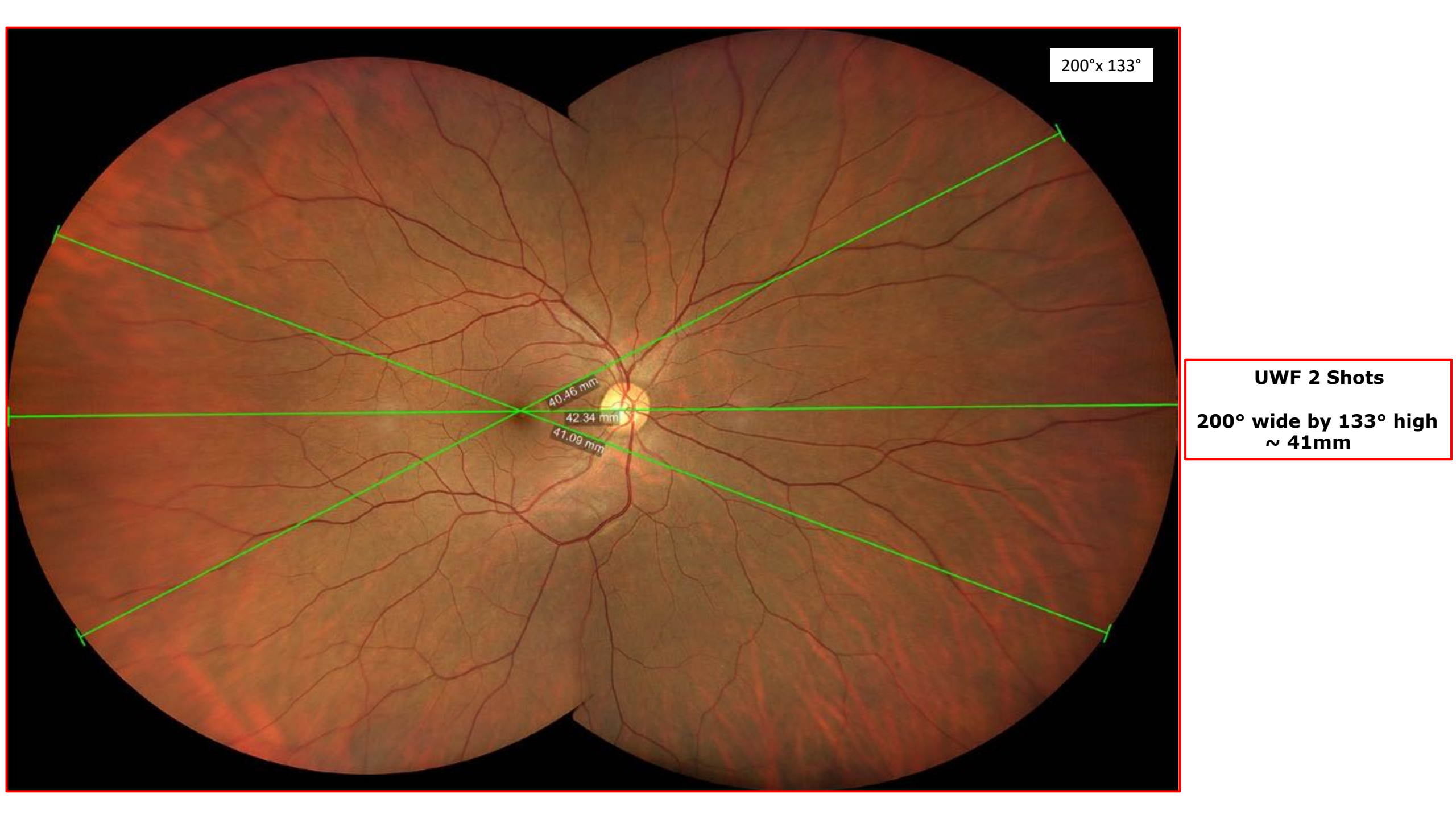
133° x 133°

27.25 mm

1 Shot WF

FoV 133°x 133°

~ 27 mm SINT



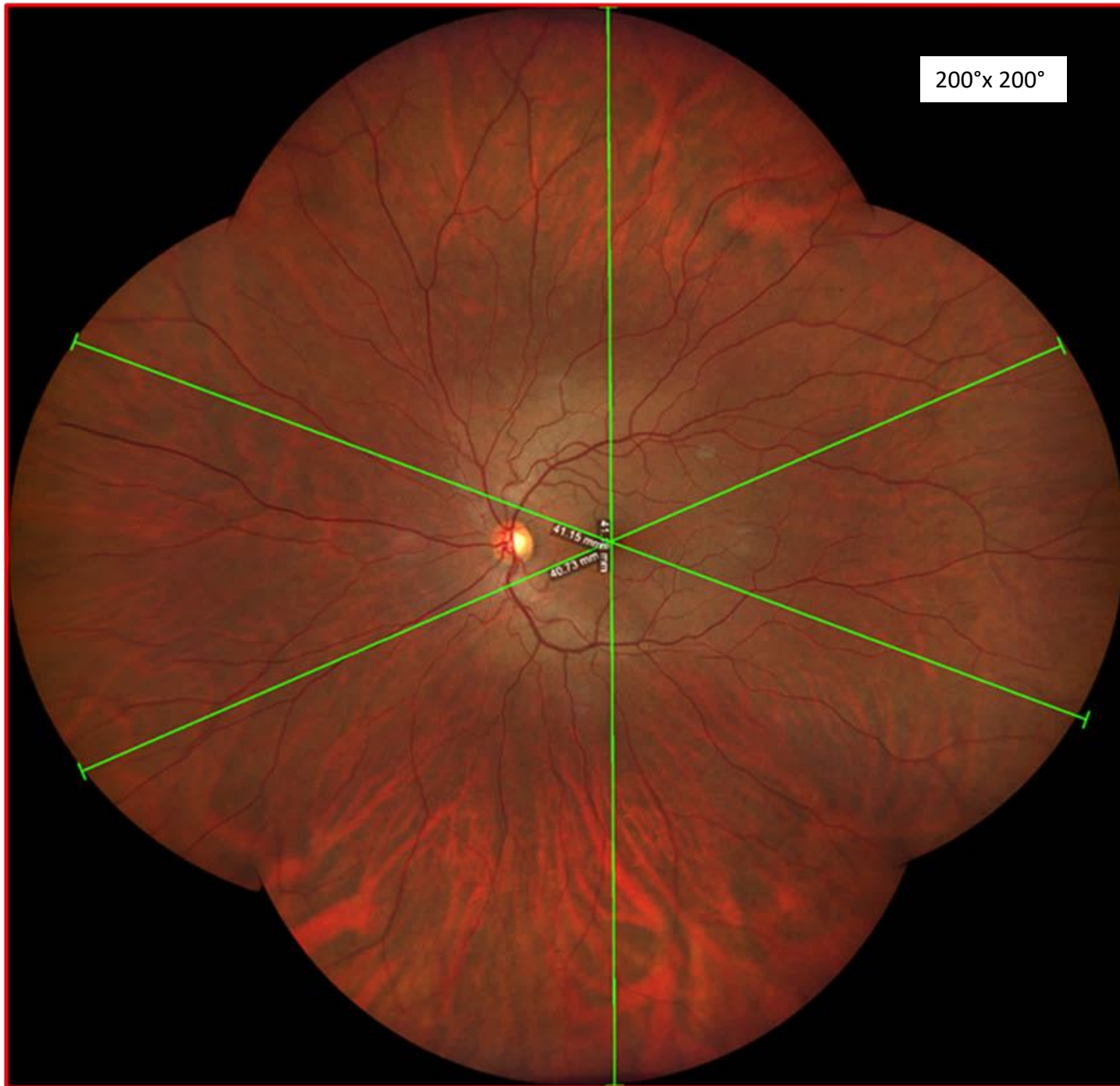
200°x 133°

40.46 mm

42.34 mm

41.09 mm

UWF 2 Shots
200° wide by 133° high
~ 41mm



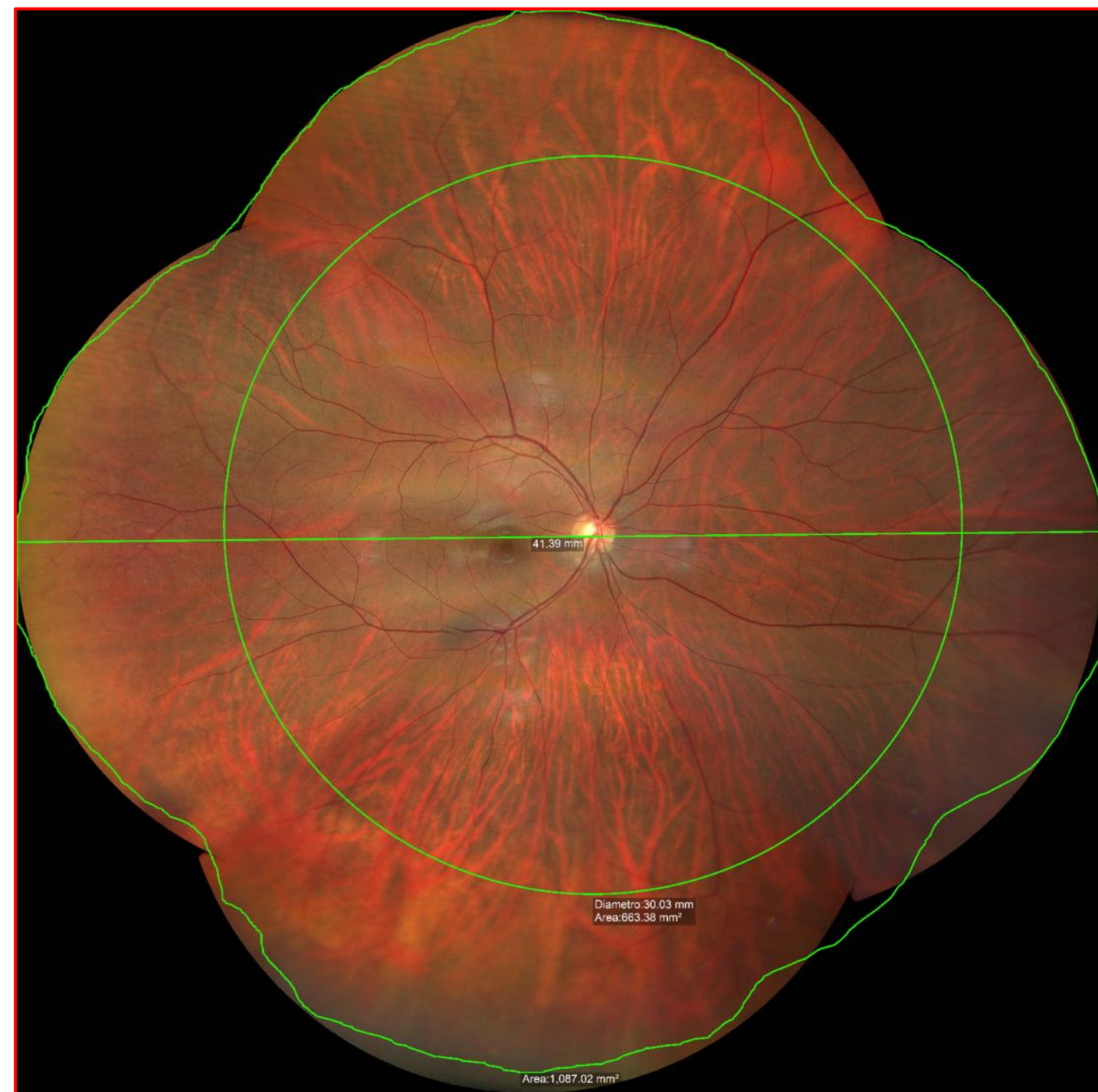
200° x 200°

UWF 4 Shots

automatic montage

FoV 200° x 200°

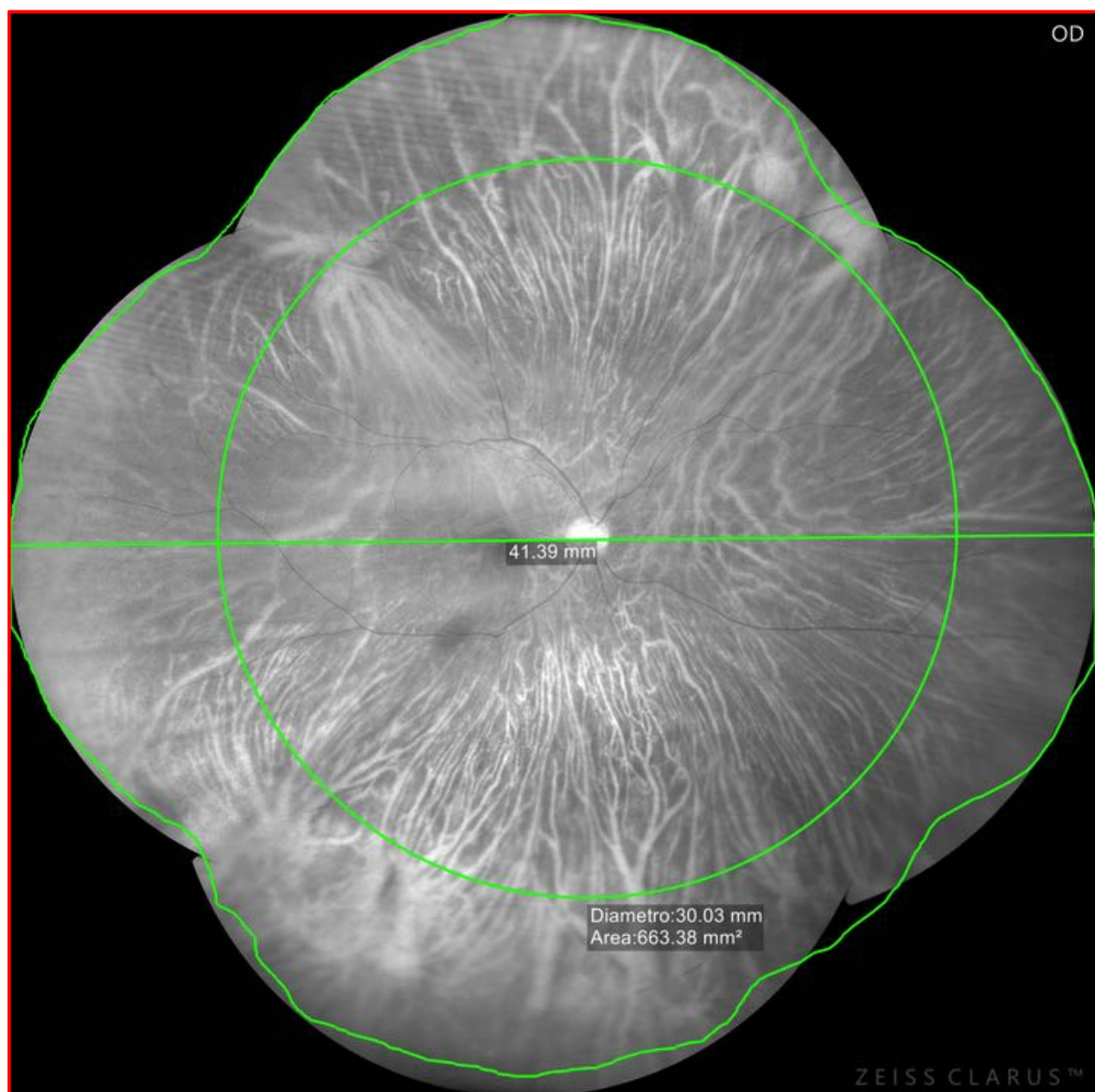
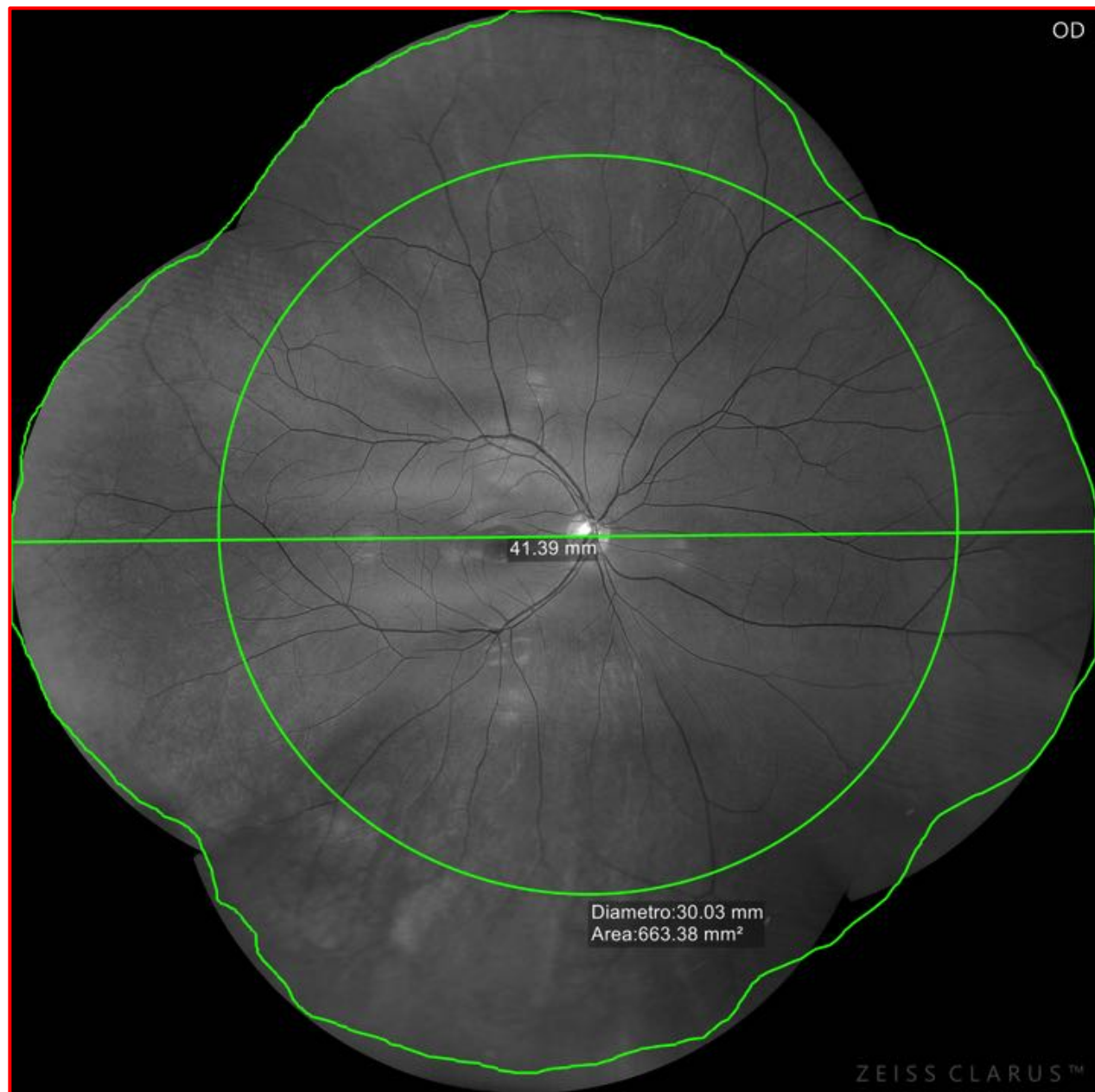
wide by tall ~ 41 mm



WF v/s UWF
vortex vein ampulla ~ 30mm
real area ± 670mm²

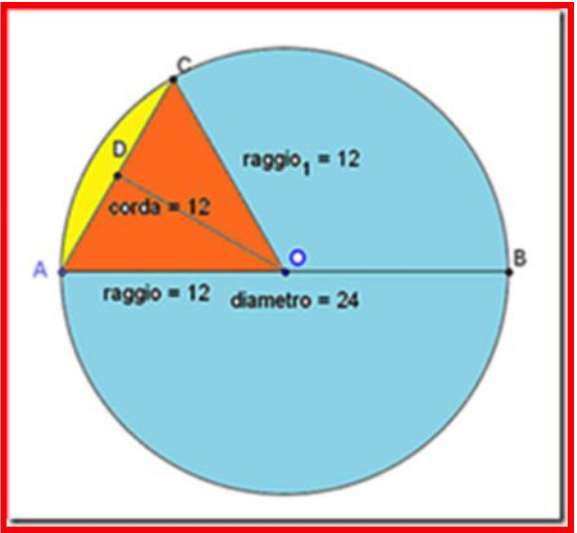
wide by tall ~ 41 mm
real area ± 1100mm²





Misure bulbo teorico Testut, Zaccheo, Bonnet, Orzalesi

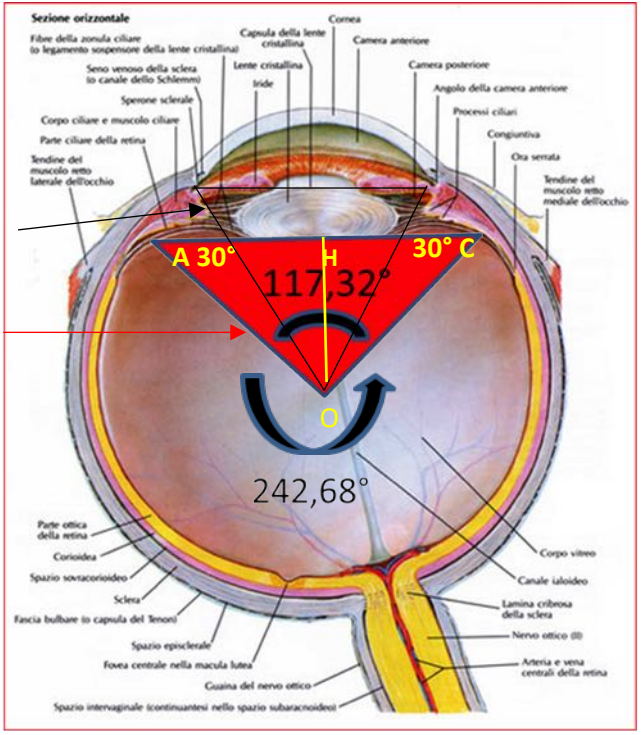
SFERA IDEALE



- AB ~ 24 mm
- AO ~ 12 mm
- AC ~ 12 mm
- AC arco ~ 12,56mm
- AOC Triangolo Equilatero ~ 60°

- Equilatero 12mmx3/60°
- Isoscele AOC 12x2/20mm 30°x2/60°

117,32° + 242,68° = 360°



Testut, Zaccheo, Bonnet, Orzalesi, le dimensioni del bulbo oculare umano sono:
 diametro trasverso 23,5 mm
 diametro verticale 23 mm
 diametro antero-posteriore 25-26 mm
 Forma ricalca un ellissoide triassiale

Diametro trasverso latero-laterale $d \sim 24\text{mm}$; raggio ideale $r \sim 12\text{mm}$

Lunghezza circonferenza $C = 2 \pi r = 2 \times 3,14 \times 12\text{mm} \sim 75.36\text{mm}$

Corpo ciliare bulbo $\sim 6\text{mm}$; 2 corpi ciliari = $2 \times 6\text{mm} \sim 12\text{mm}$

Corda bianco-bianco $\sim 12\text{mm}$

Arco corneale sotteso alla corda bianco- bianco $\pm 1/6 C = 75,36/6 \sim 12,56\text{mm}$

Arco circ- ora serrata/ora serrata $12,56+2 \text{ corpi ciliari}=12,56+12 \sim 24,56\text{mm}$

Lungh. lineare seg. post. fotografabile $75,36\text{mm} - 24,56\text{mm} \sim 50,80\text{mm}$

Seg. ant. non fotografabile in $\varphi 75,36\text{mm} : 360 = 24,56 : X \sim 117,32^\circ \frac{\cos 30^\circ \sqrt{3}}{2}$

Seg. post. fotografabile in $\varphi 360^\circ - 117,32^\circ \sim 242,68^\circ$

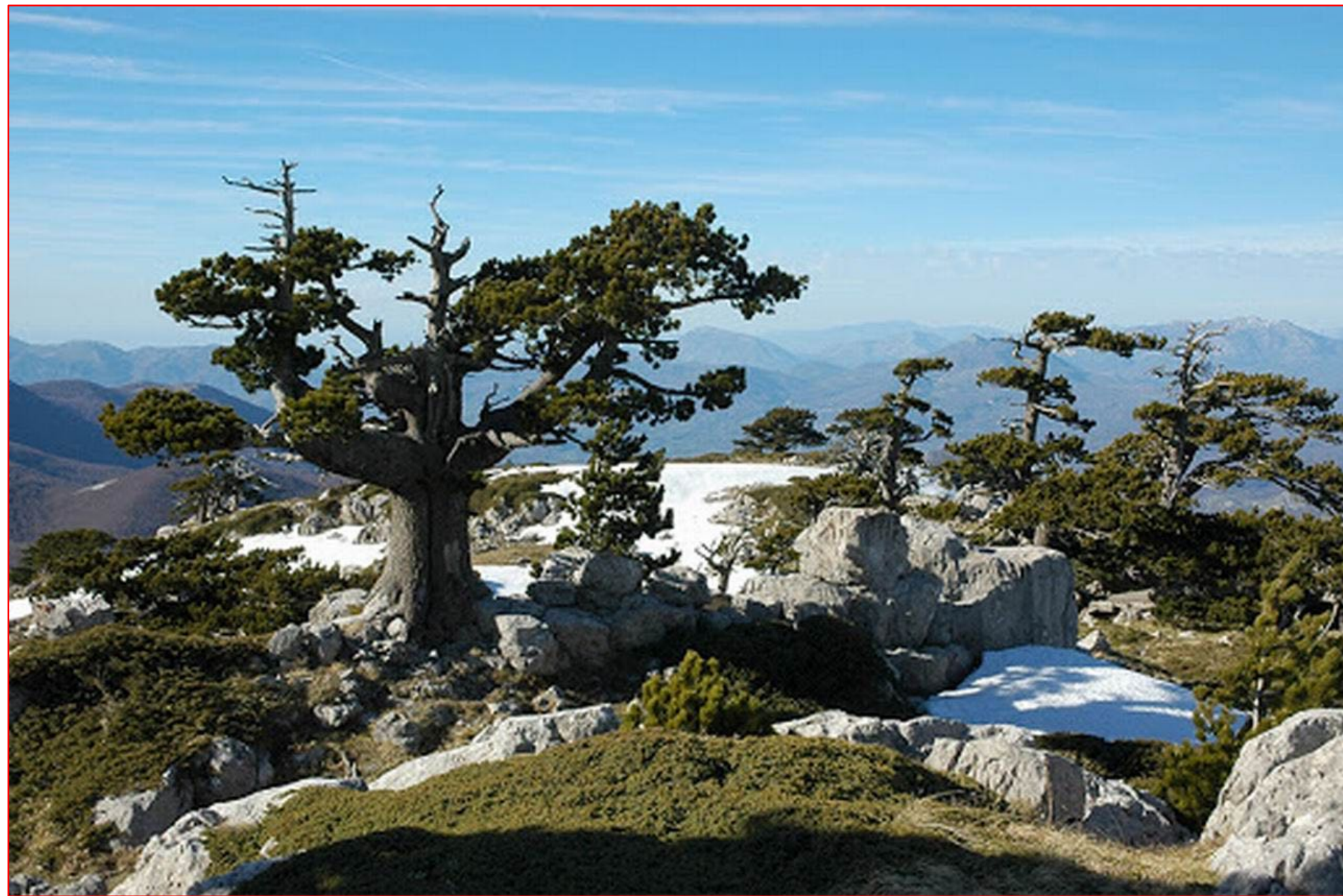
$AO=CO =12$; $AC = 2 \times AH$; $AH = AO \cos 30^\circ = 12 \cos 30^\circ = 6\sqrt{3}$; $AC = 2 \times 6\sqrt{3} \pm 20,5\text{mm}$

$OH = \sqrt{AO^2 - AH^2} = \sqrt{12^2 - 10^2} = \sqrt{144 - 100} = \sqrt{44} = 6,7\text{mm}$

Superficie area retinica sfera perfetta $4 \times \pi r^2 = 4 \times 3,14 \times 12^2 \sim 1808\text{mm}^2$

Superficie area retinica emisfera perfetta $\frac{1}{2} 4 \times \pi r^2 \sim 1808/2 \sim 904\text{mm}^2$

Seg. post fotografabile in $\text{mm}^2 1808 : 360^\circ = X : 242,68 \sim 1218,8\text{mm}^2$





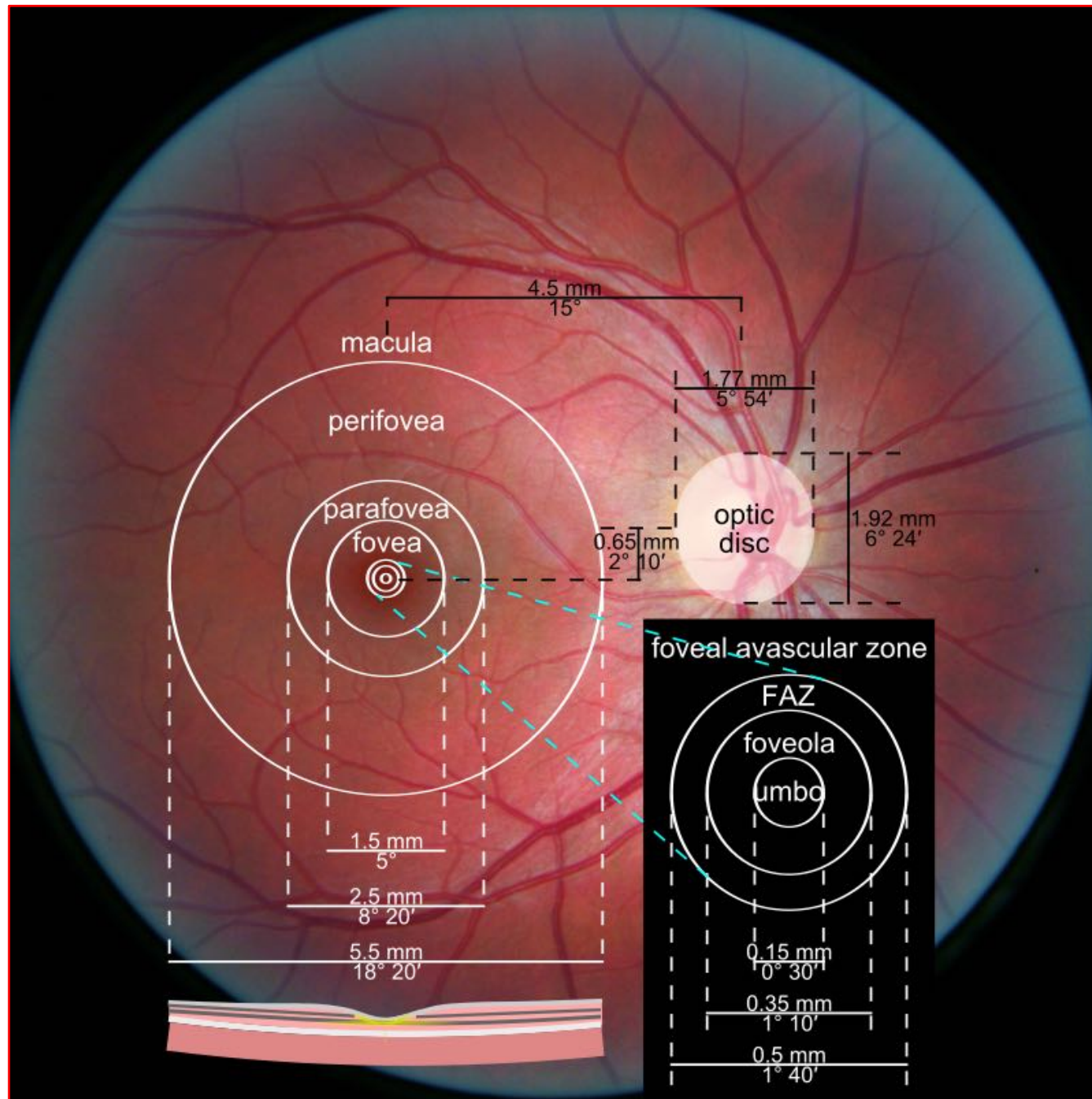
**UWF 6 Shots
semiautomatic montage
wide by tall ~ 50mm**

**central circle
~ FoV 45°
diameter ±16mm (radius ± 8mm)
area ~ 200 mm²**

**site to site full imaging
FoV 242° ≠ 267°**

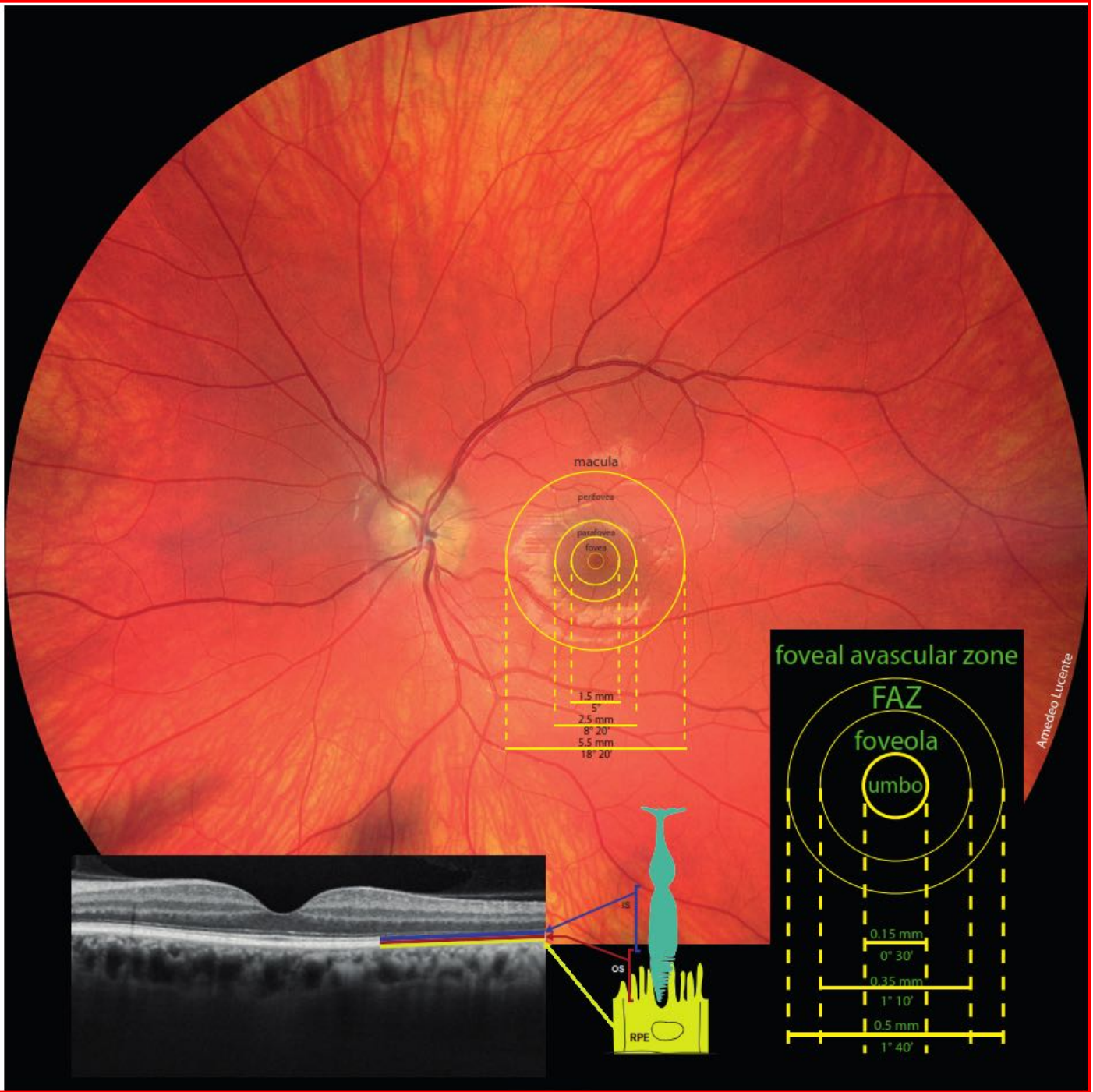
real imaging ~ 1400mm²

1808:100=1400:X; X = 77,5%



by Wikipedia

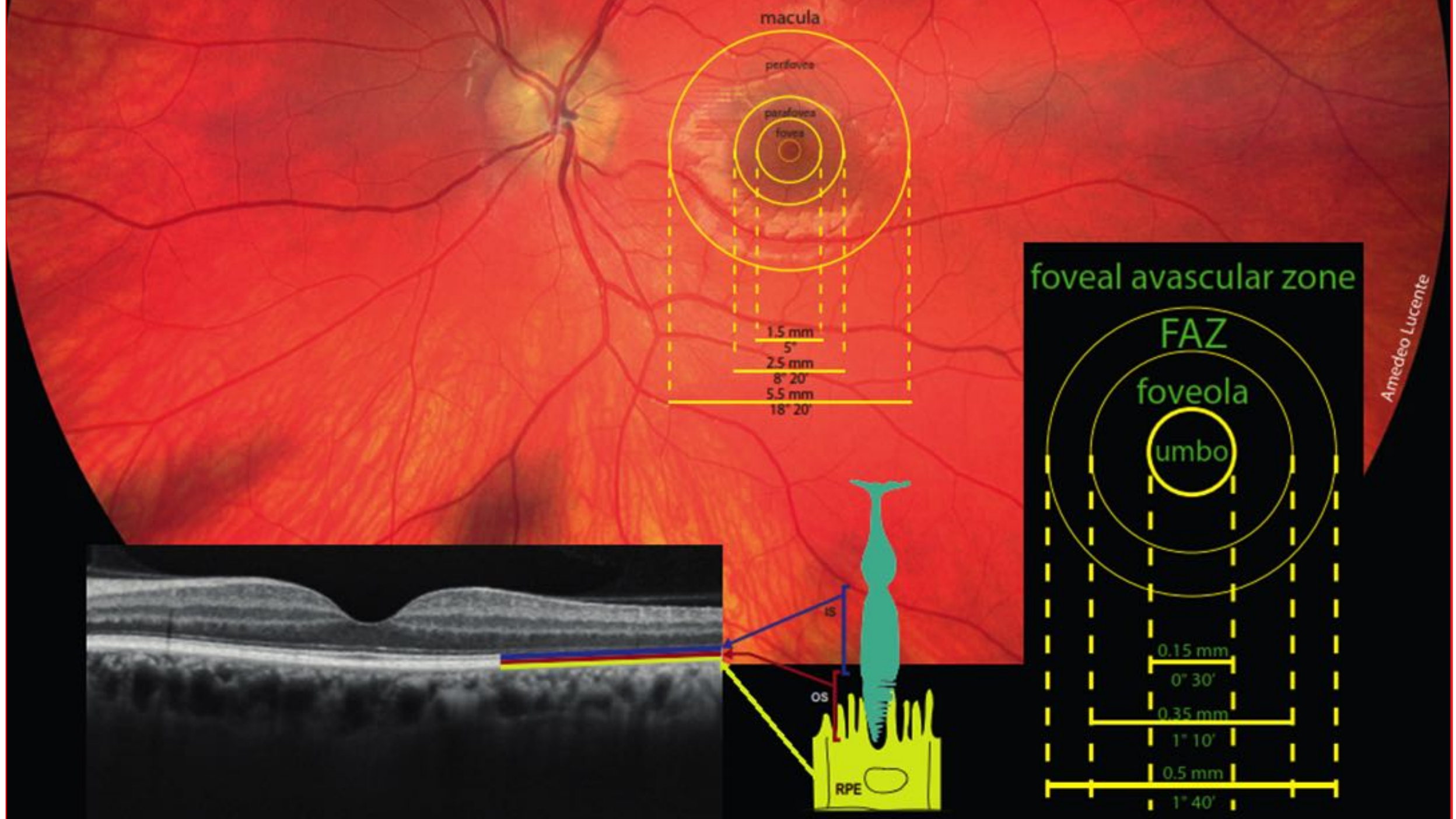
by Clarus Zeiss



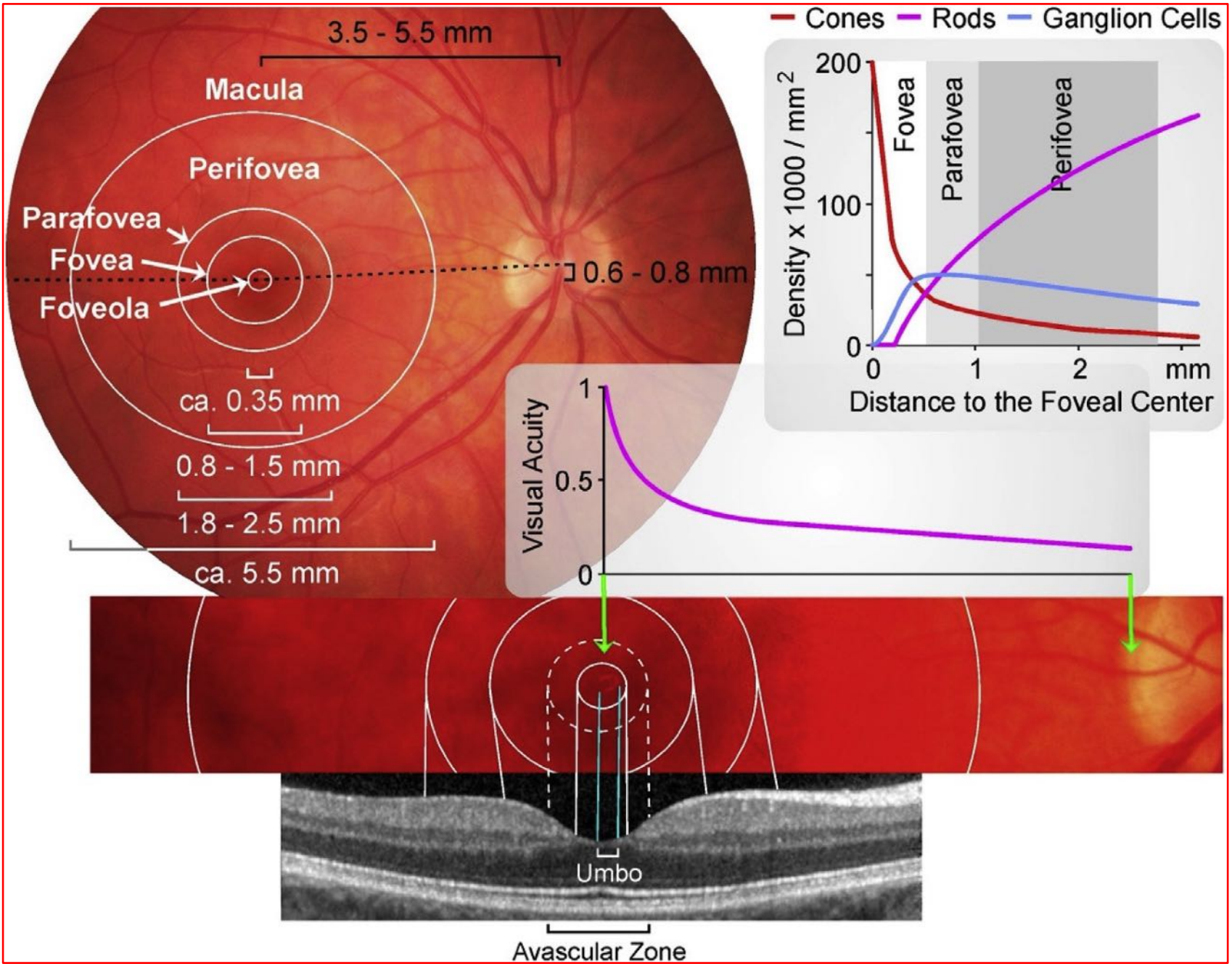
Macula	
Diameter	5,5mm
Radius	2,75mm
Area $\pi r^2 =$	23,8mm ²

Parafovea	
Diameter	2,5mm
Radius	1,25mm
Area $\pi r^2 =$	4,90mm ²

Fovea	
Diameter	1,5mm
Radius	0,75mm
Area $\pi r^2 =$	1,77mm ²

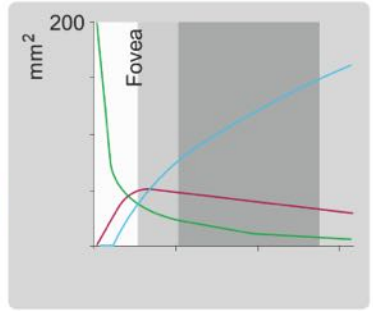
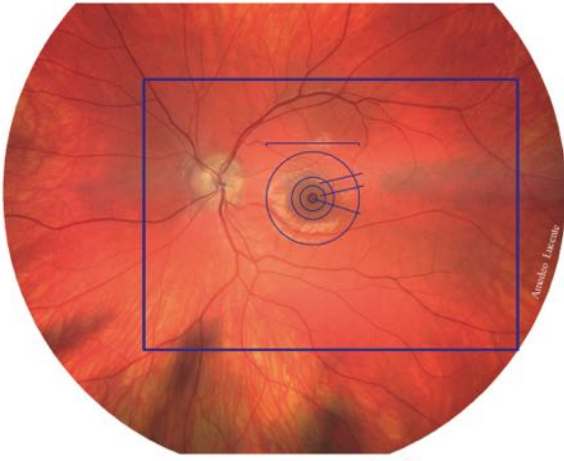


Amedeo Lucente

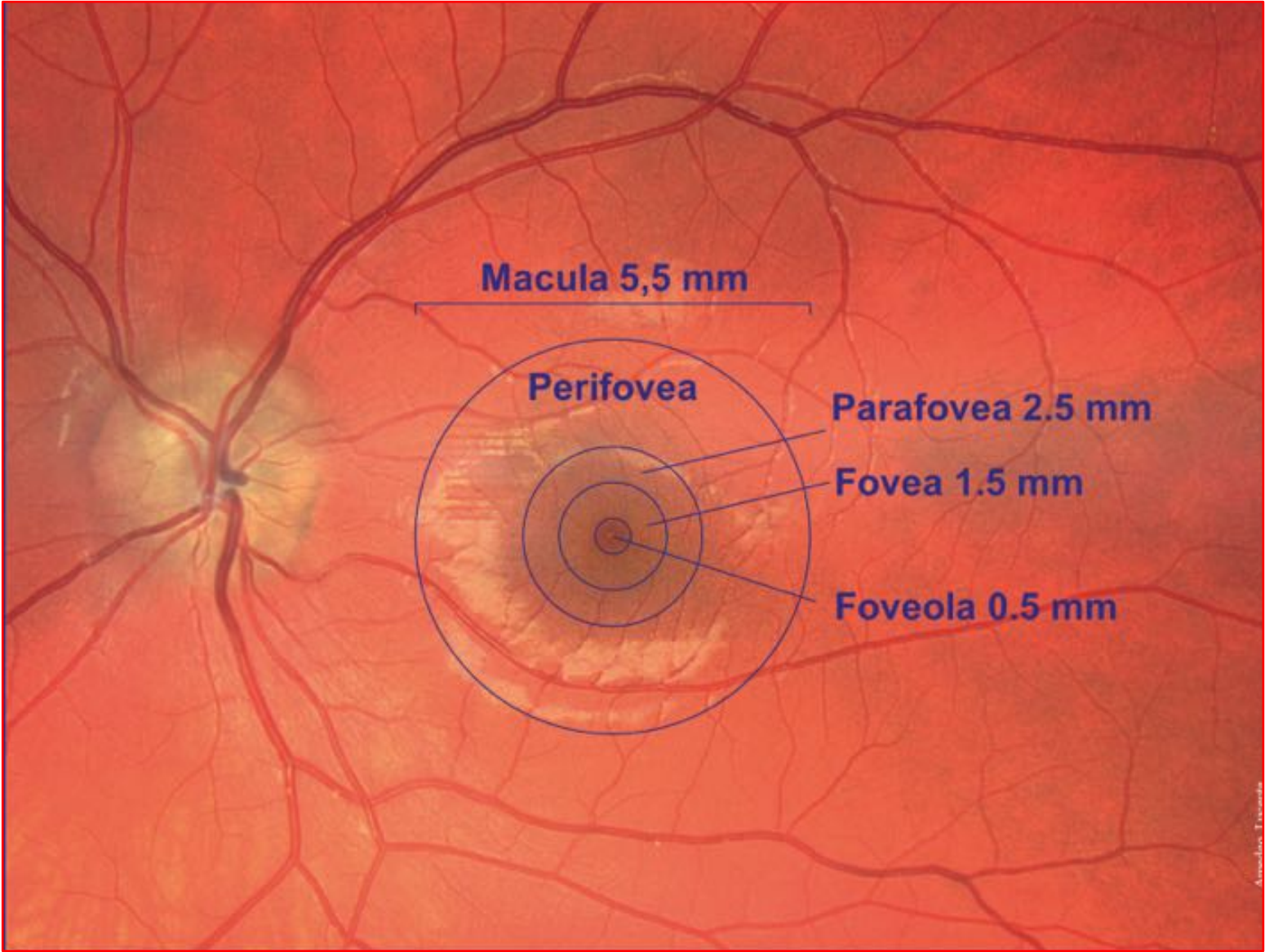
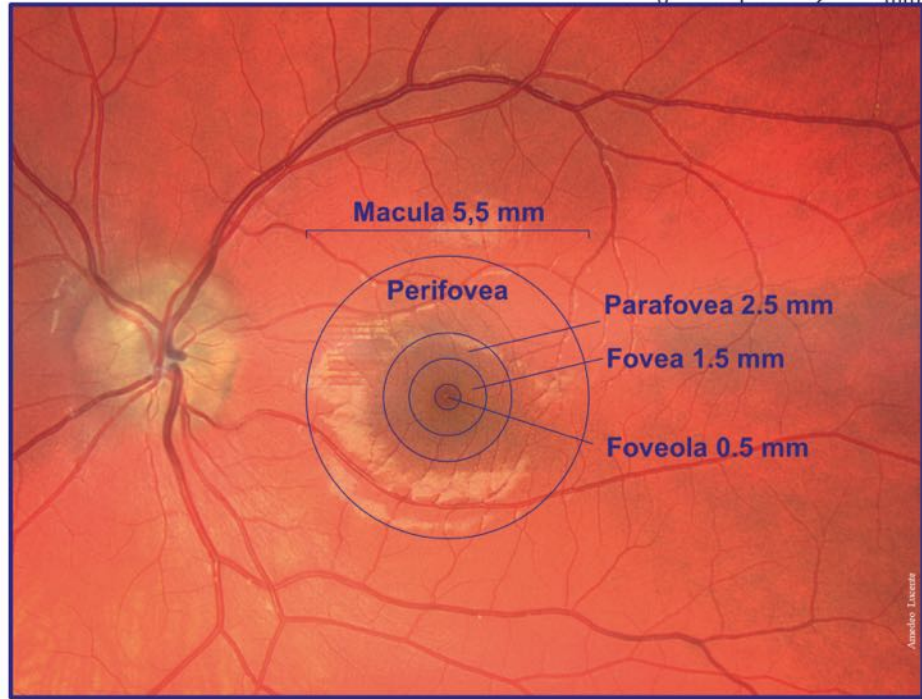


by **Andreas Bringmann et al.**
Progress in Retinal and Eye Research
Vol 66, September, 2018, Pages 49-84

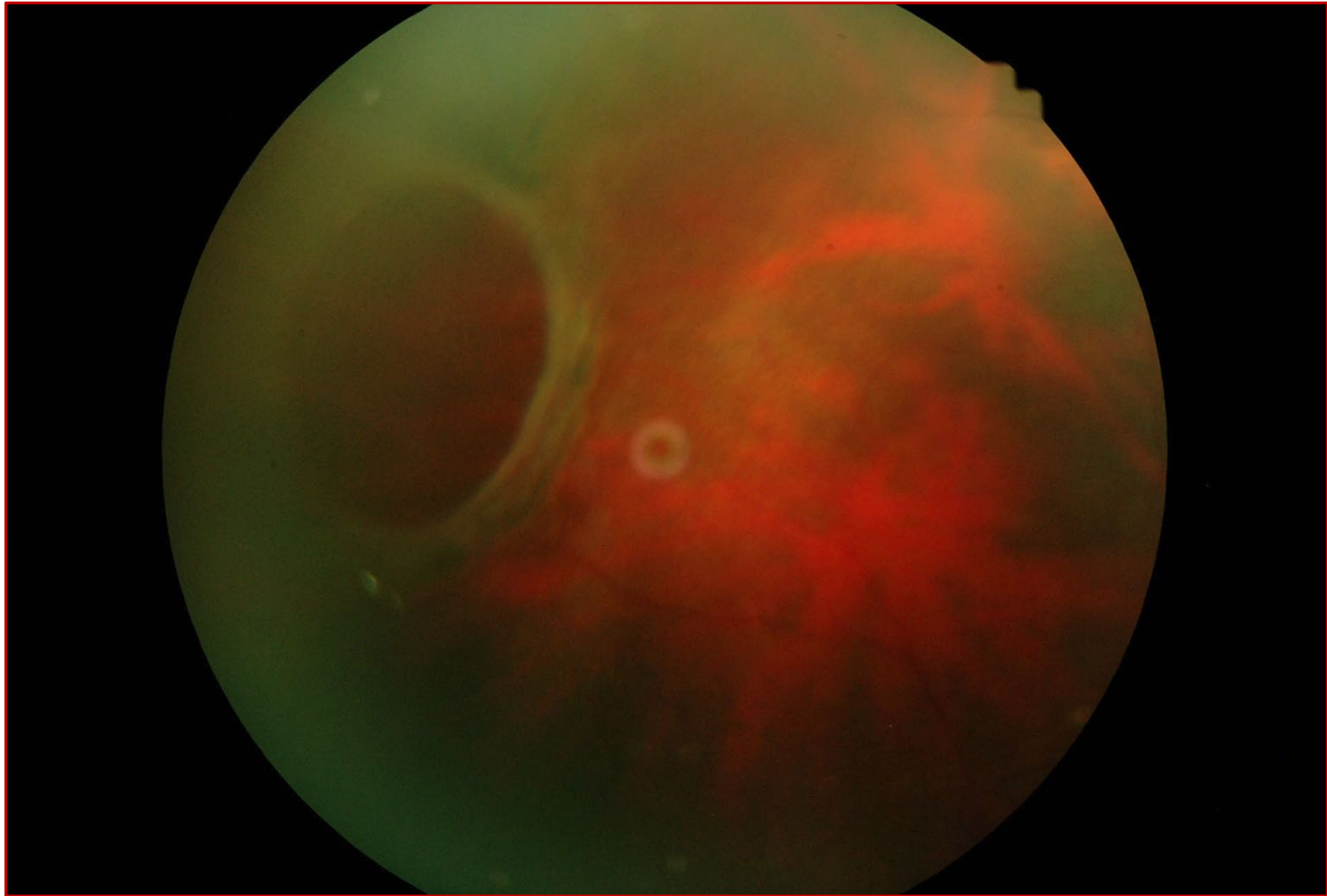
by Clarus Zeiss

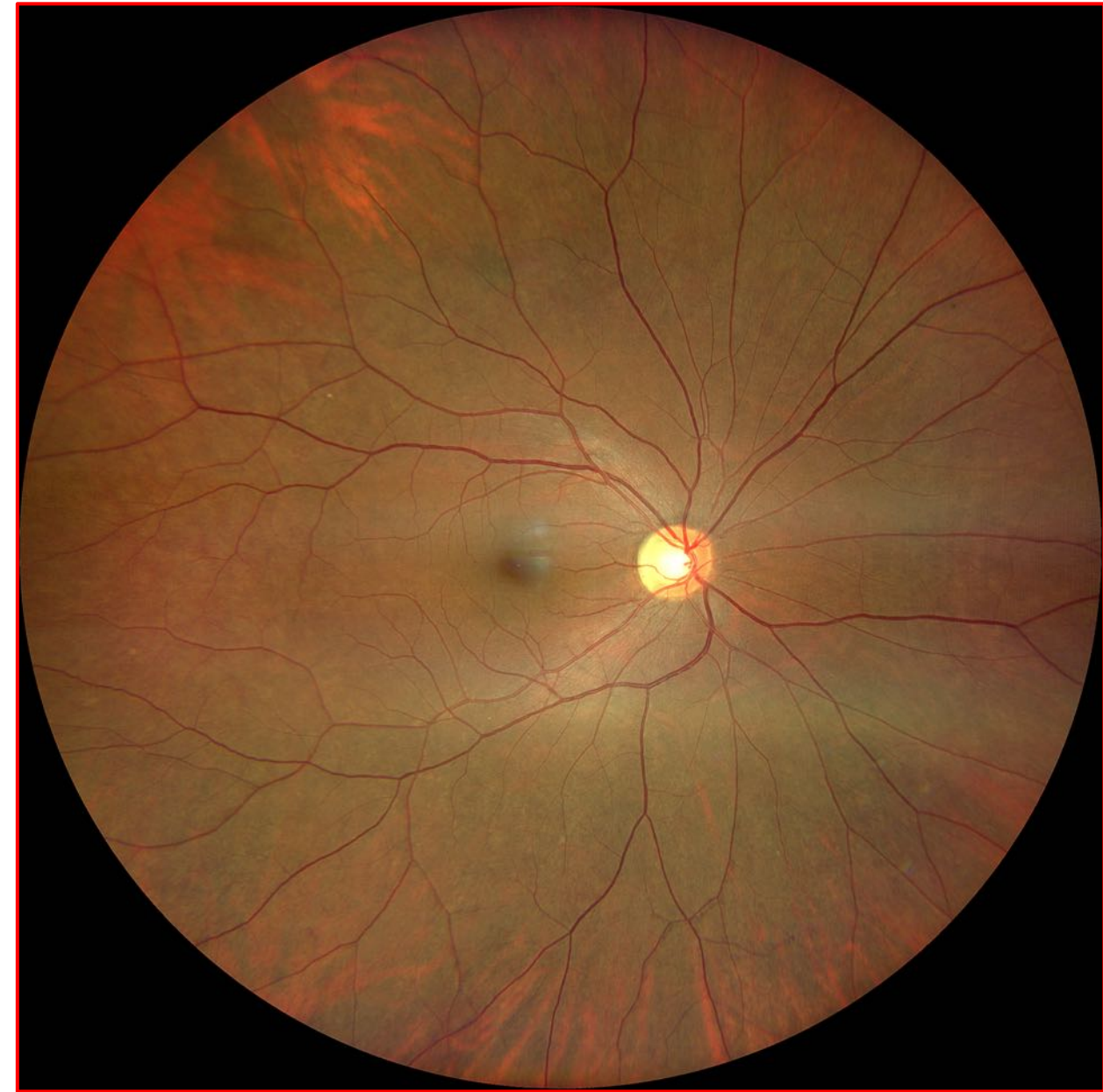


0 1 2 mm









*Foro retinico
periferico gigante:
Consensus Conference*

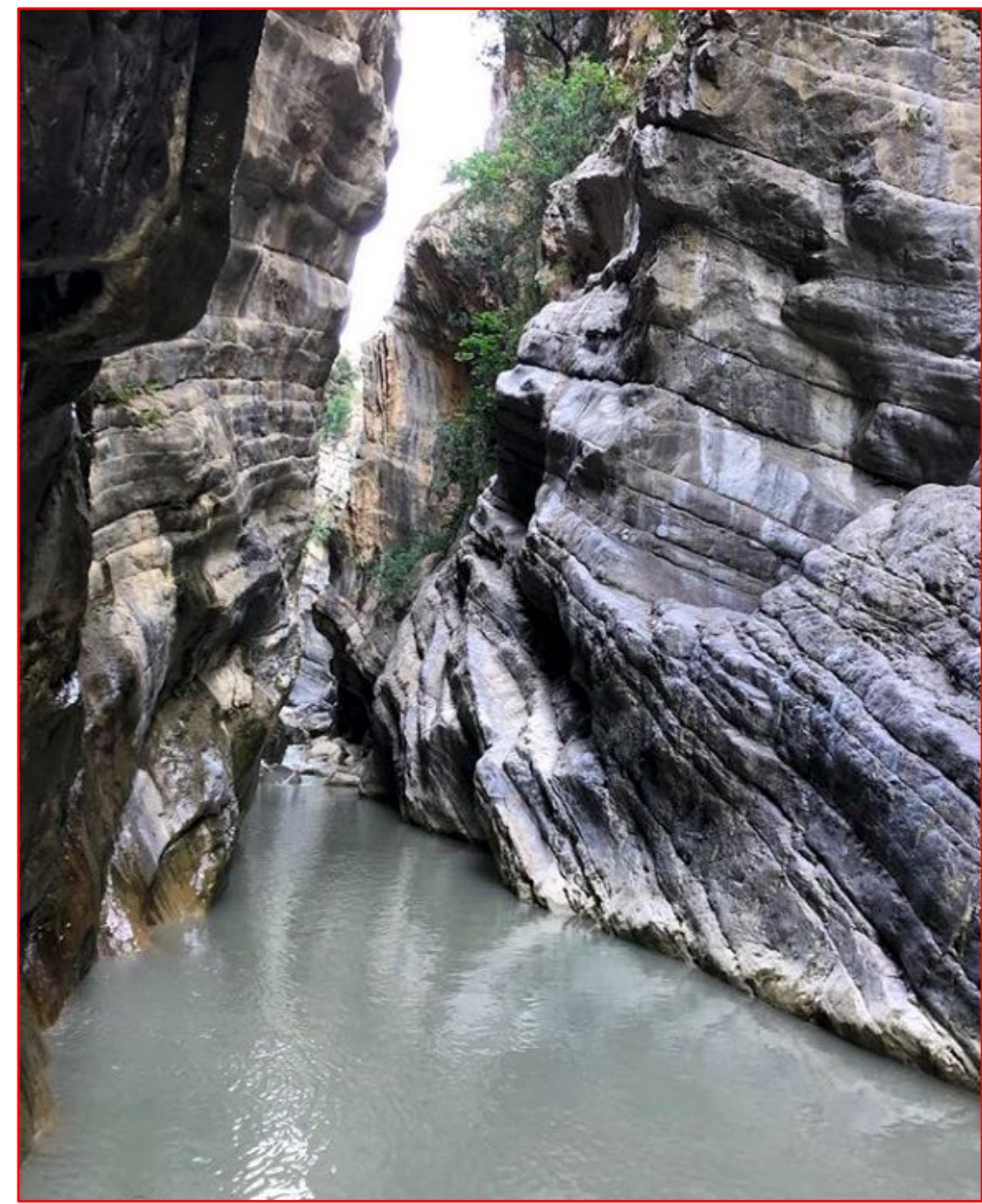
di Amedeo Lucente

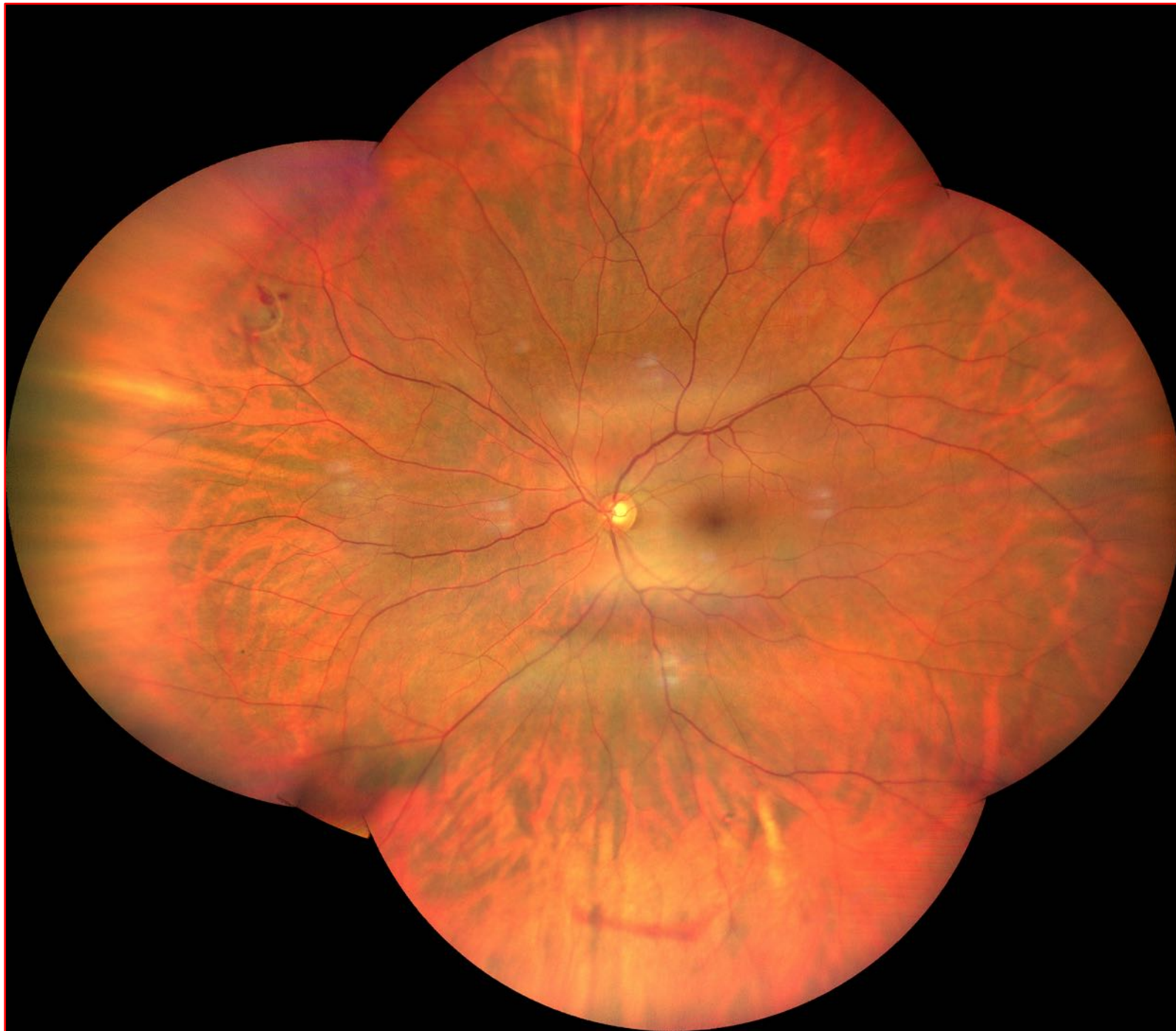
Contributors:

P. Arpa - Monza
T. Avitabile - Catania
C. Azzolini - Varese
F. Bandello - Milano
A. Berarducci e A. Laborante – S G. Rotondo
M. Borgioli - Macerata
F. Boscia - Sassari
C. Carbonara - Roma
E. dell’Omo - Campobasso
R. di Lauro - Napoli
C. Girkin – Birmingham US
T. Micelli Ferrari - Acquaviva delle Fonti
A. Montericcio - Trapani
C. Panico - Torino
A. Pece - Milano
V. Petitti - Roma
P. Pintore e P. Patteri - Alghero
G. Querques - Milano
V. Ramovecchi - Macerata
A. Rapisarda - Catania
M. Rispoli - Roma
S. Rizzo - Firenze
G. Scorcio - Catanzaro



**Giant
peripheral
retinal
hole**

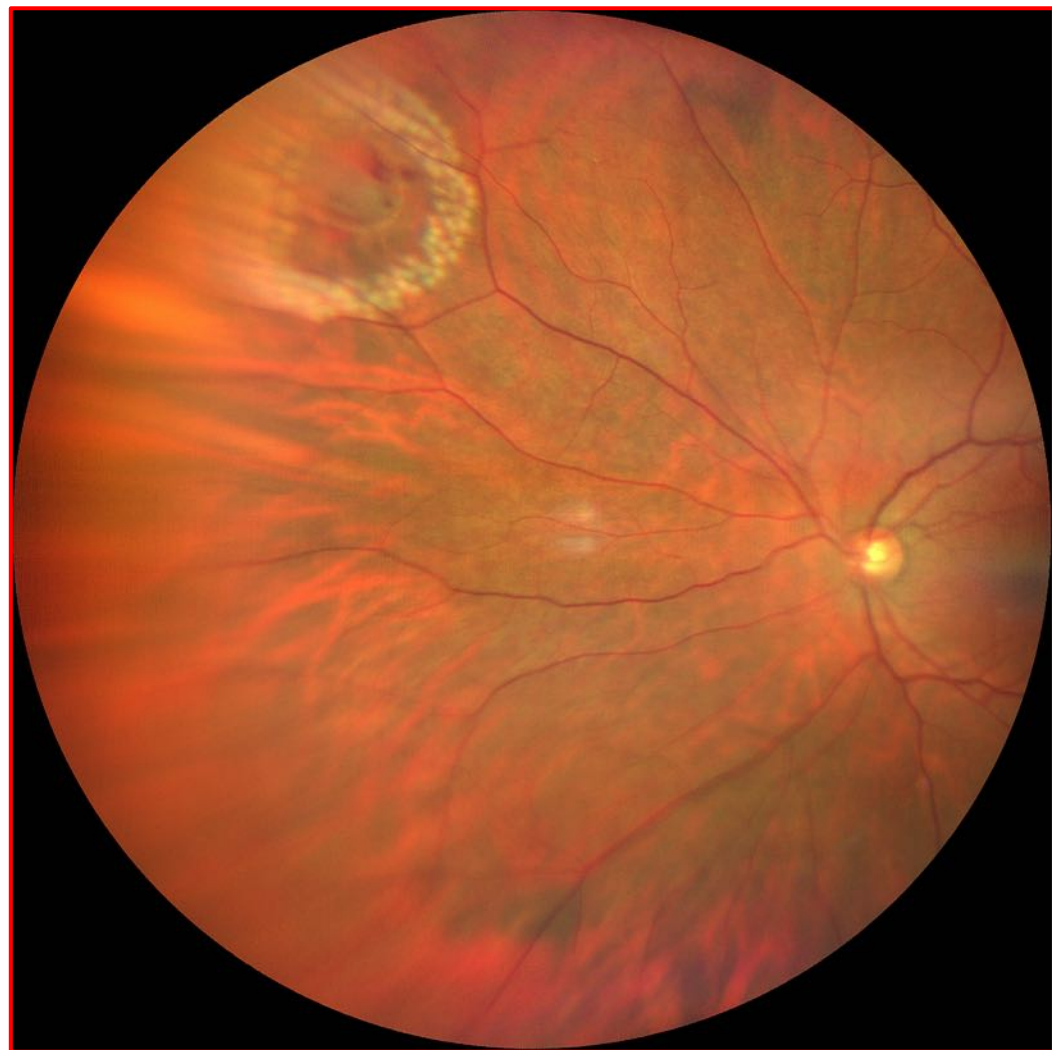




4 shots
Horseshoe-shaped retinal tear
with emovitreo six o'clock

Horseshoe-shaped retinal tear: before and after argon laser treatment

1 shot
2 shots



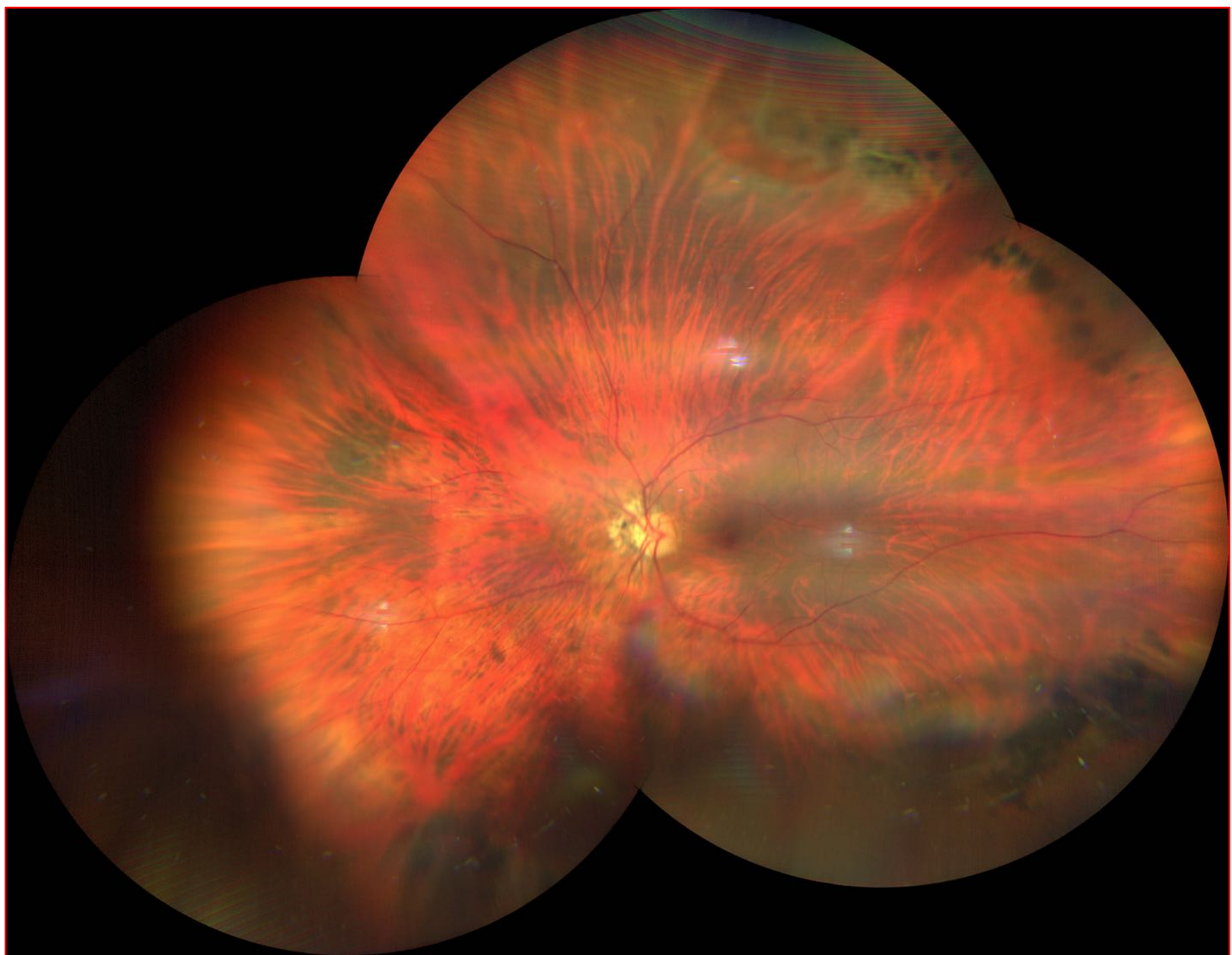
Start 30/11/20
21/01/21

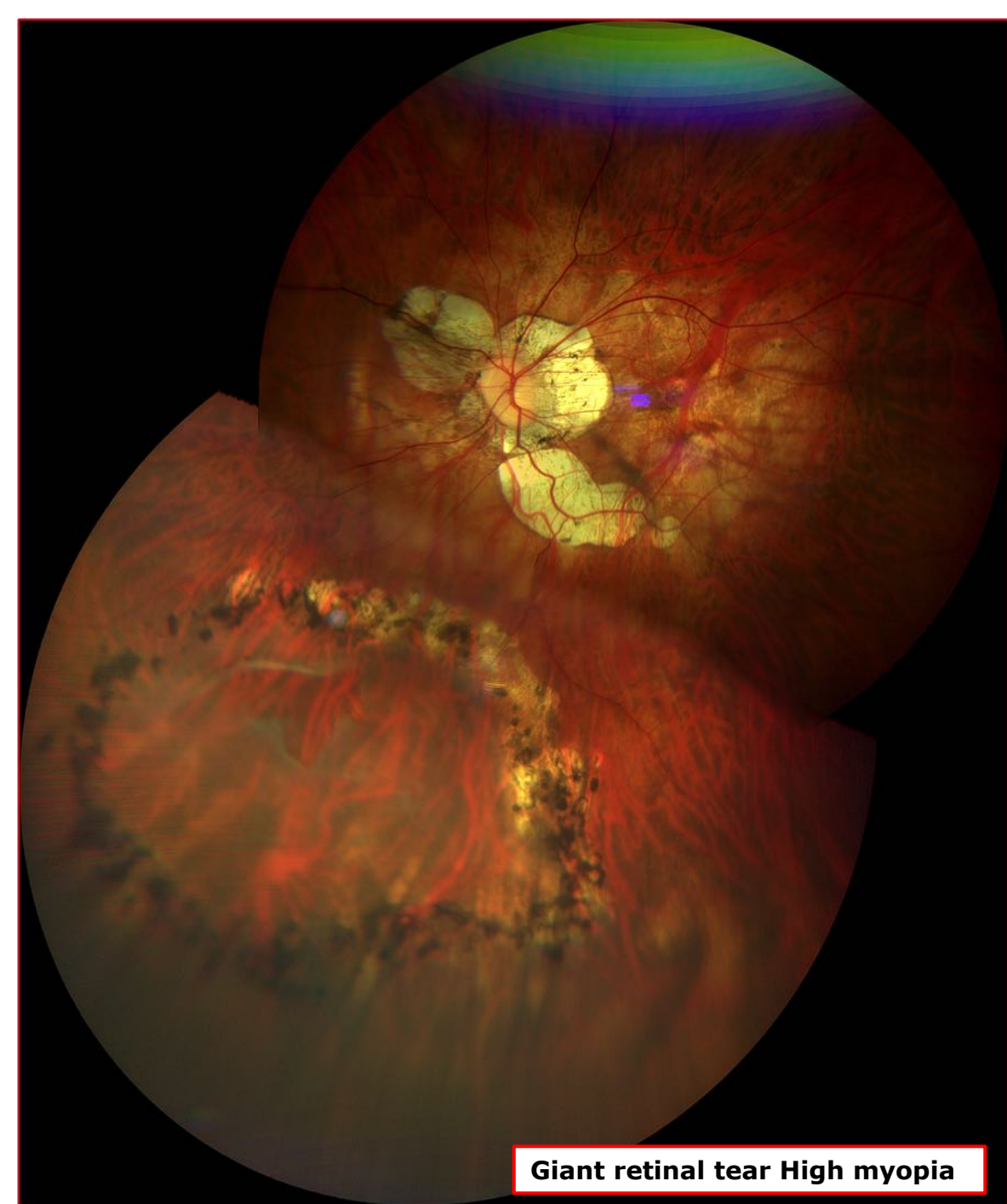
25/01/21

Argon Laser treatment horseshoe-shaped retinal tear follow-up after hemovitreus

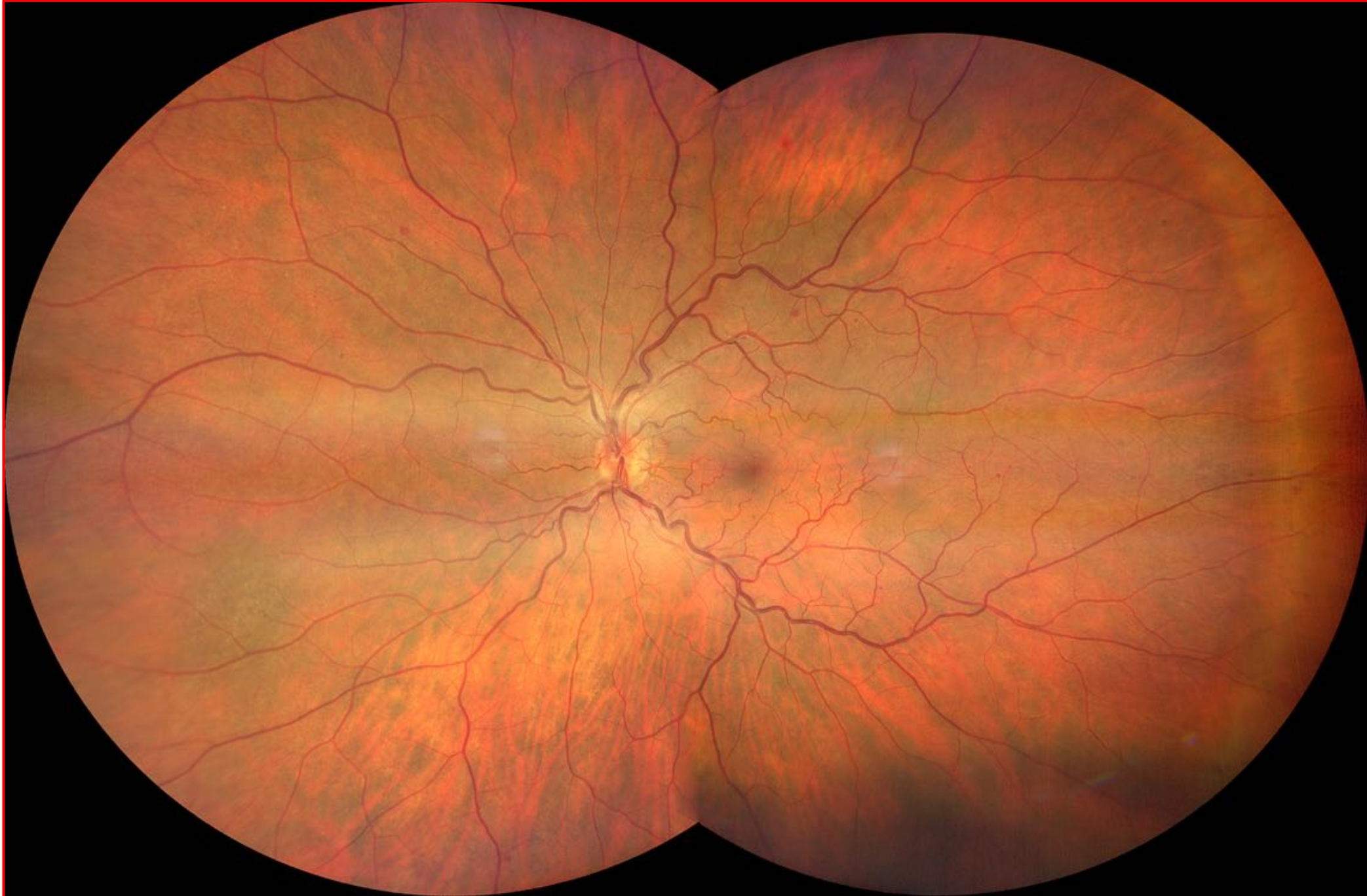












**Hypertensive
vasculopathy**



**Incipient CRVO
Central Retinal
Vein Occlusion**

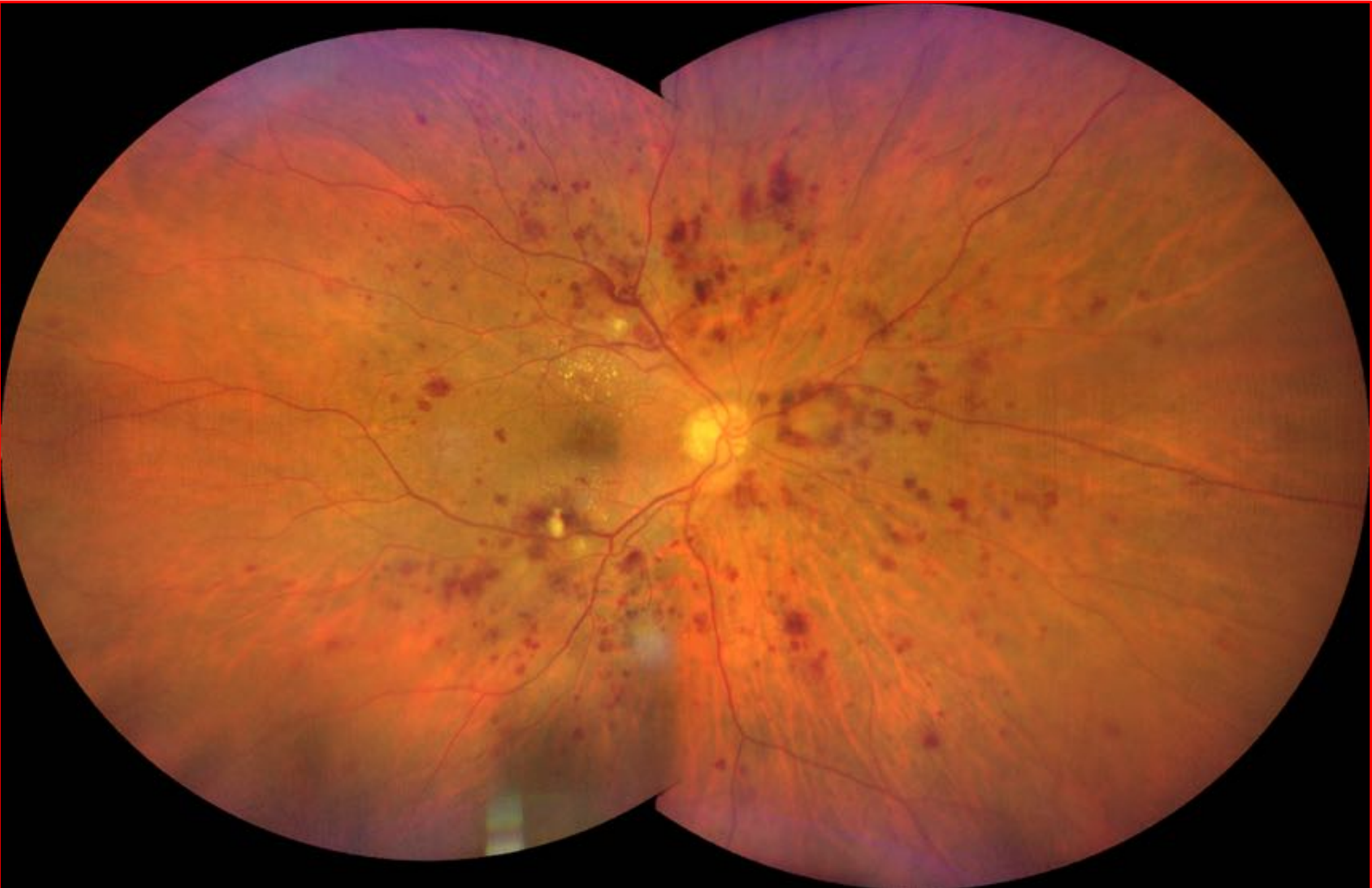
Visus 10/10



RVO
Retinal Vein
Occlusion
5.2/1000

CRVO
Central Retinal
Vein Occlusion
0.80/1000

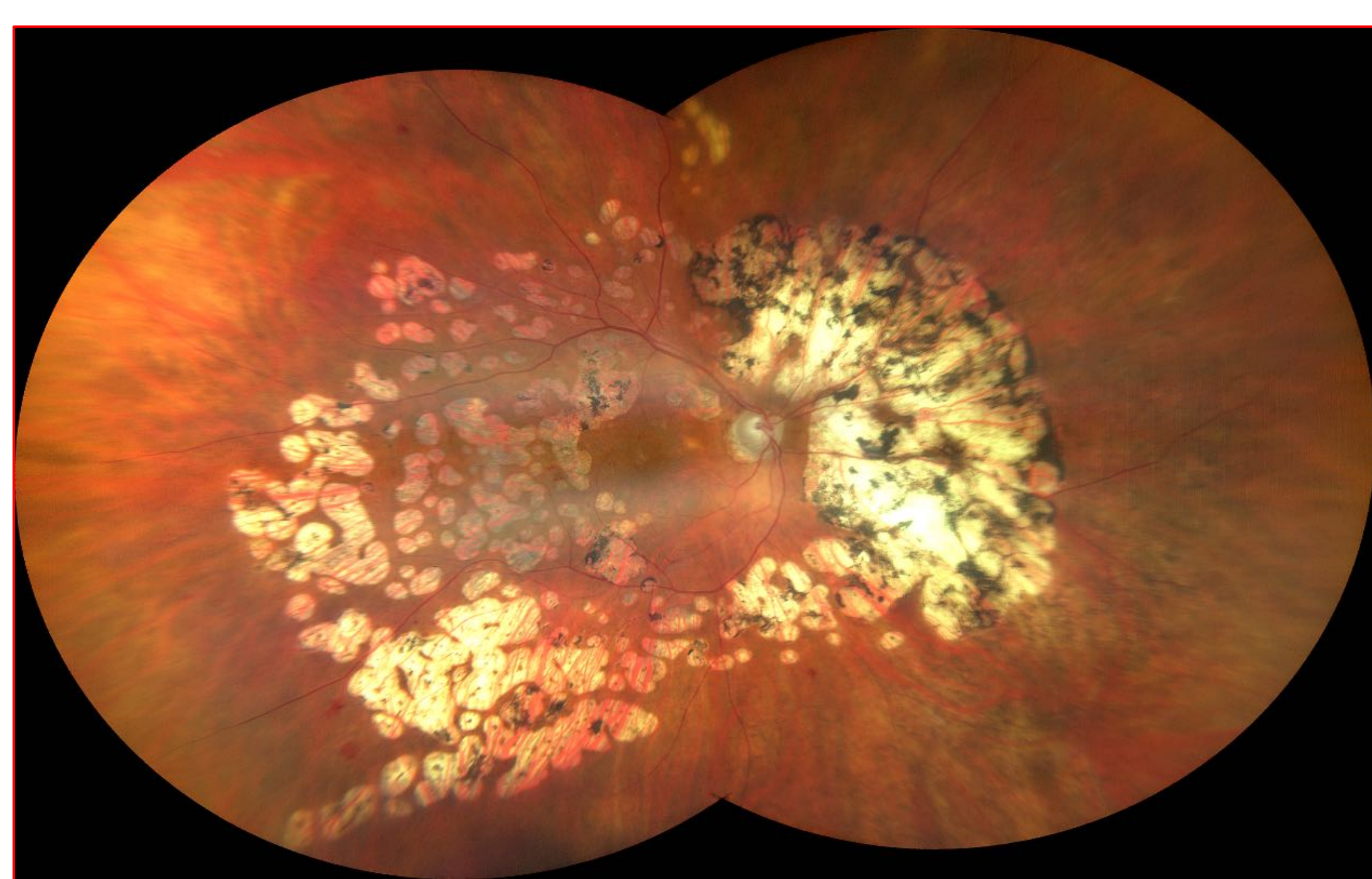
BRVO
Branch Retinal
Vein Occlusion
4.42/1000

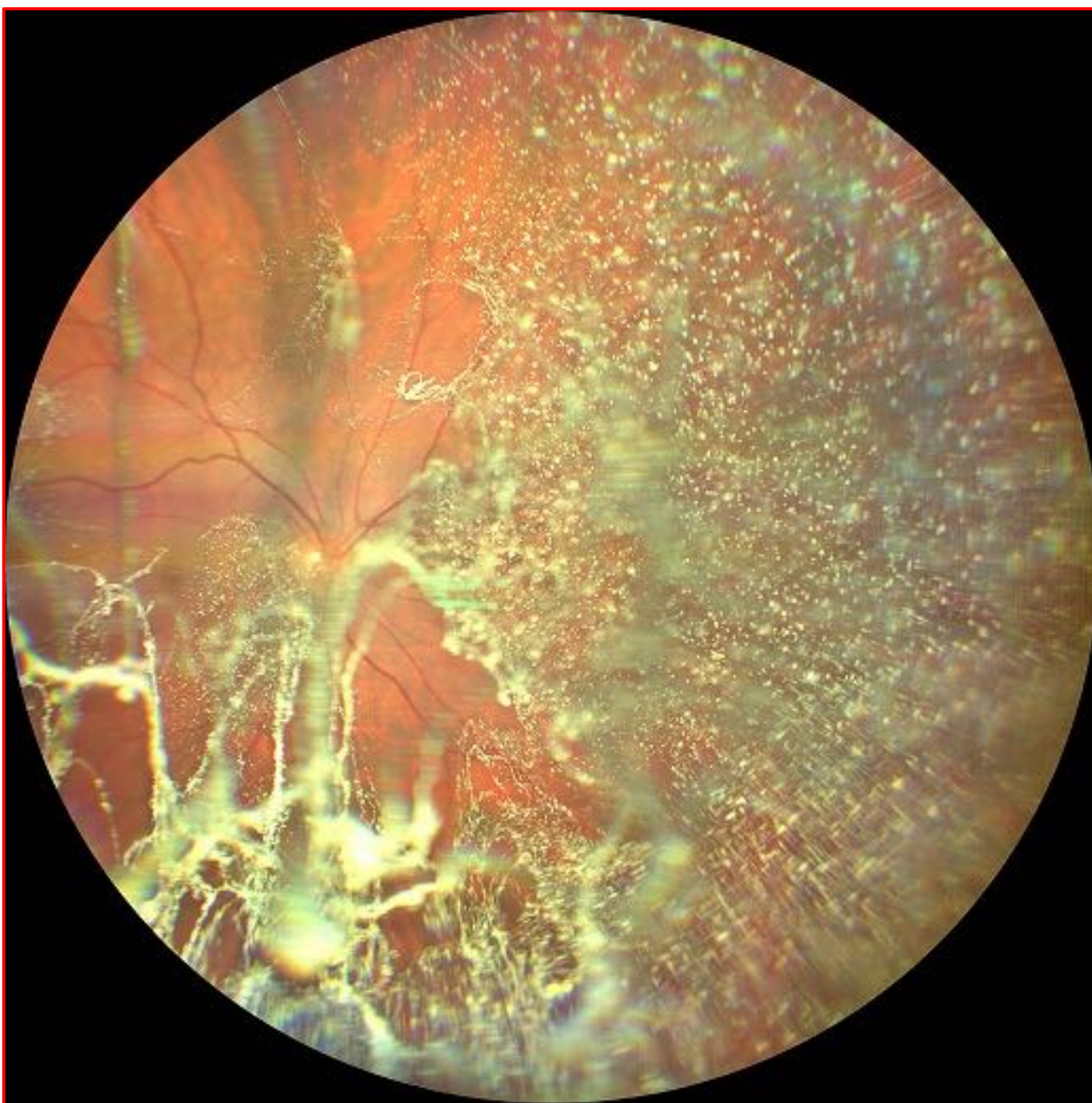


**Background
Diabetic
Retinopathy
v/s HR-PDR
High-Risk
Proliferative
Diabetic Retinopathy**



**Diabetic
Retinopathy
Excessive
Argon Laser
Treatment**



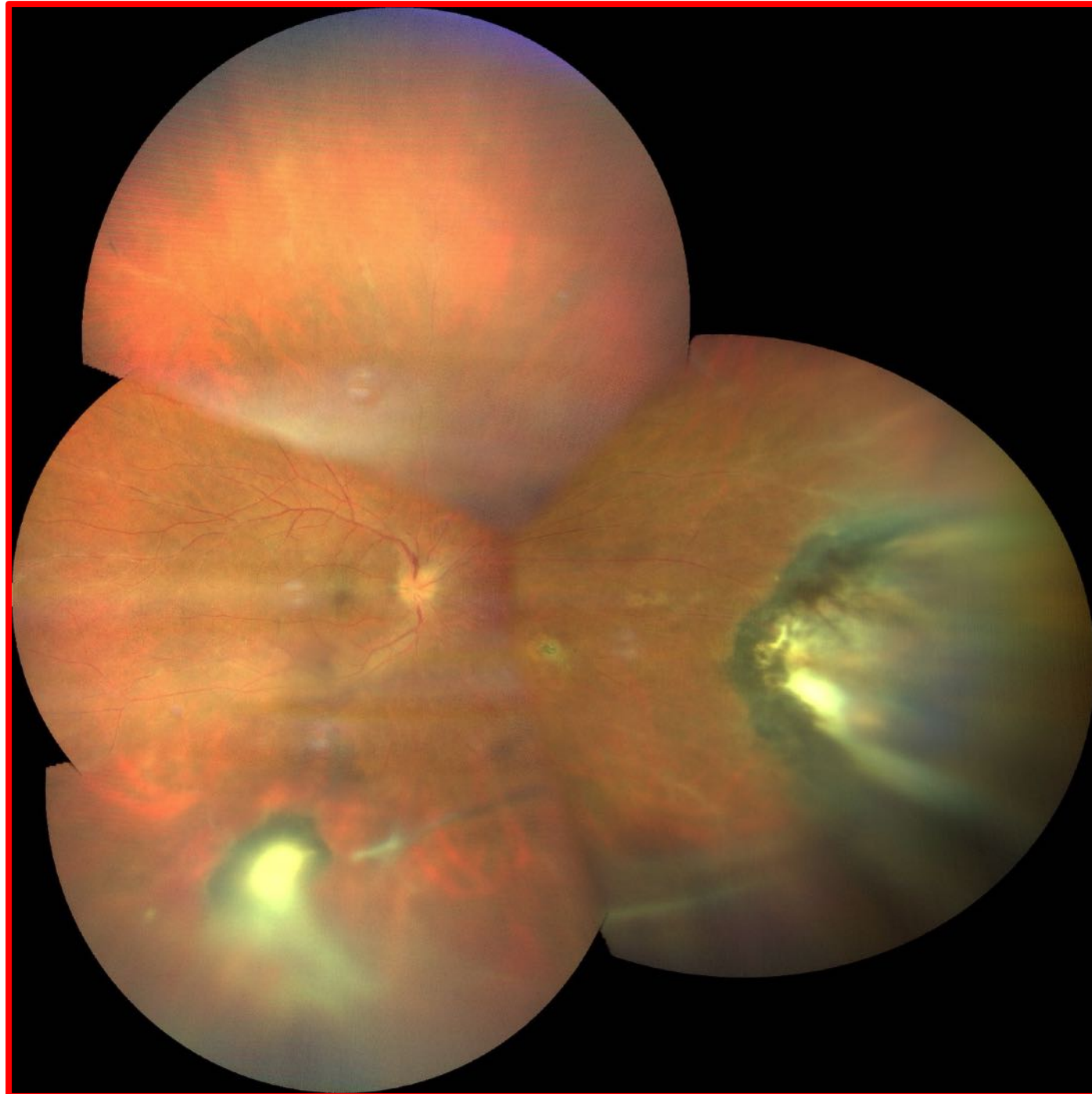


Asteroid vitreopathy
Prevalenza 0,15%-0,9%
Unilaterale 75%
calcio-fosfolipidi

Sinchisi: cristalli di colesterolo
cholesterolis bulbi



Calabria Scoprire



TOXO Recidiva

Giovane maschio
Buona salute
Primo episodio 20 aa fa

Seconda osservazione, settembre 2020

Visus 4-5/10, tyndall +, cellule +
iperemia congiuntiva bulbare +

Accertamenti sistemici di routine

Terapia d'attacco: Prednisolone 100 mg/die a scalare (terapia iniziale 80 mg al Moorfields Eye Hospital, Carlos Pavesio)

Atropina 1% x 2 v die

Betametasona + Cloramfenicolo collirio x 6 v die

Clindamicina 1.200 mg/die a scalare

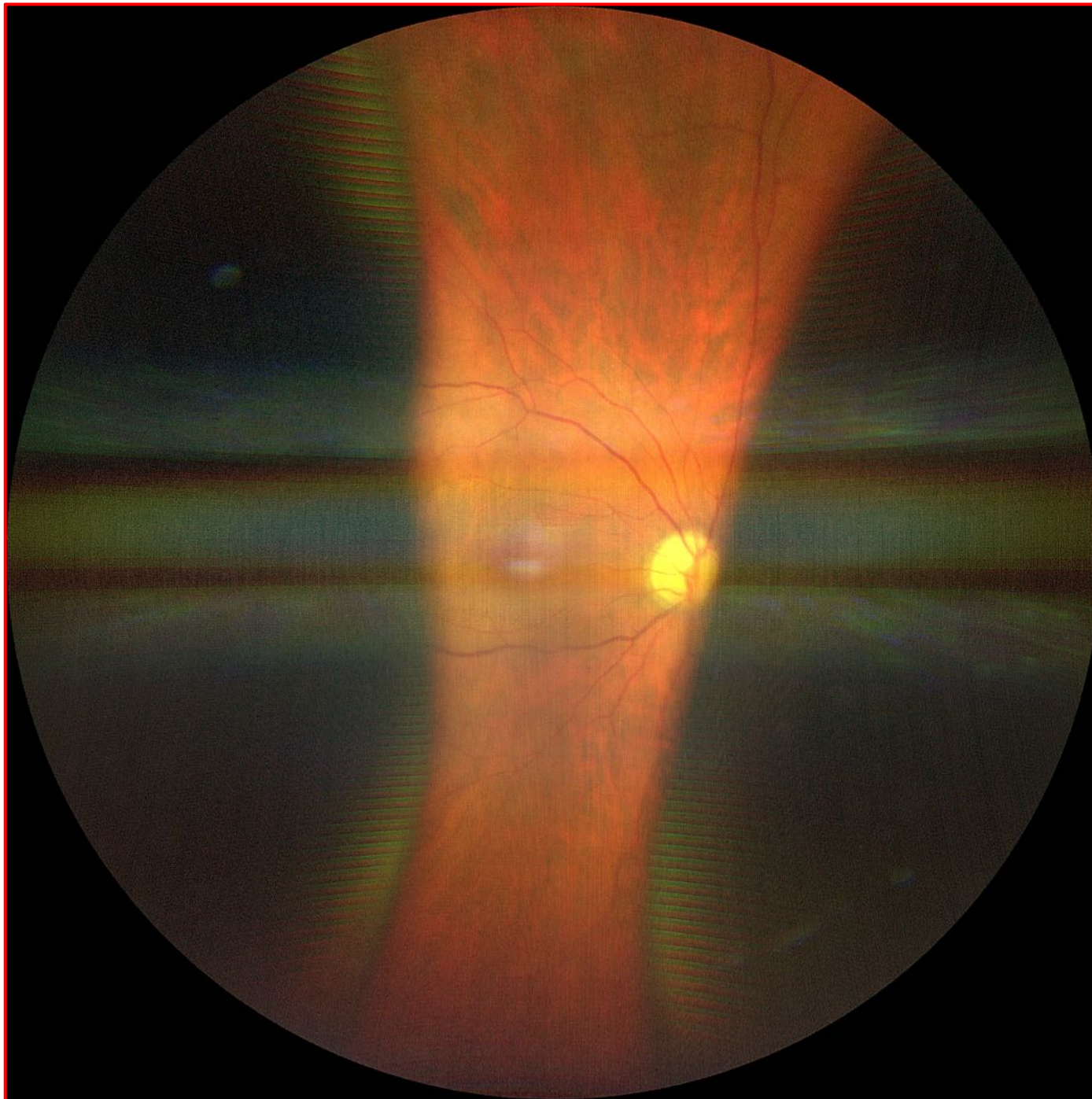
Protezione gastrica



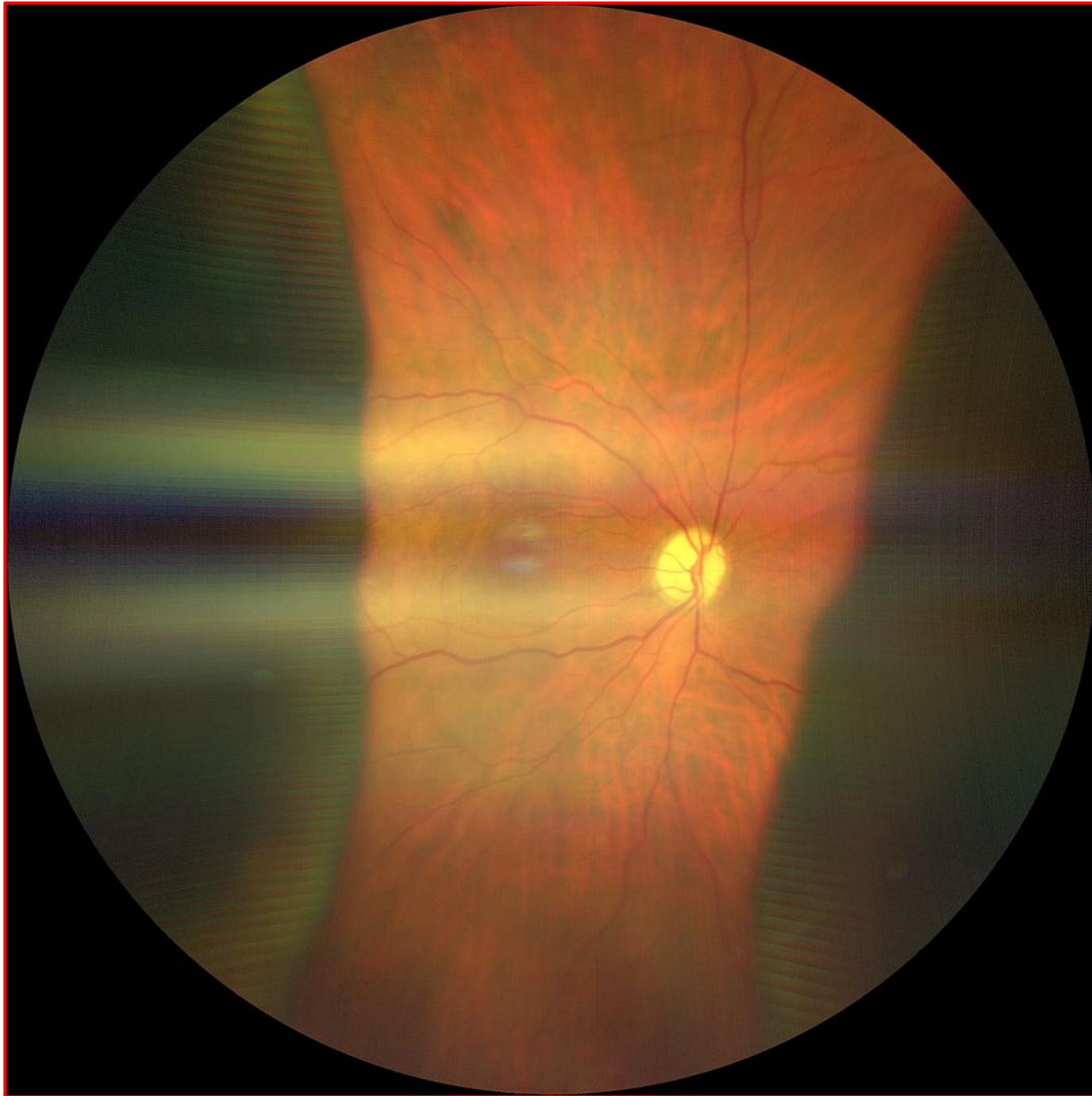
Dopo 2 mesi di terapia



Peripheral chorioretinitis



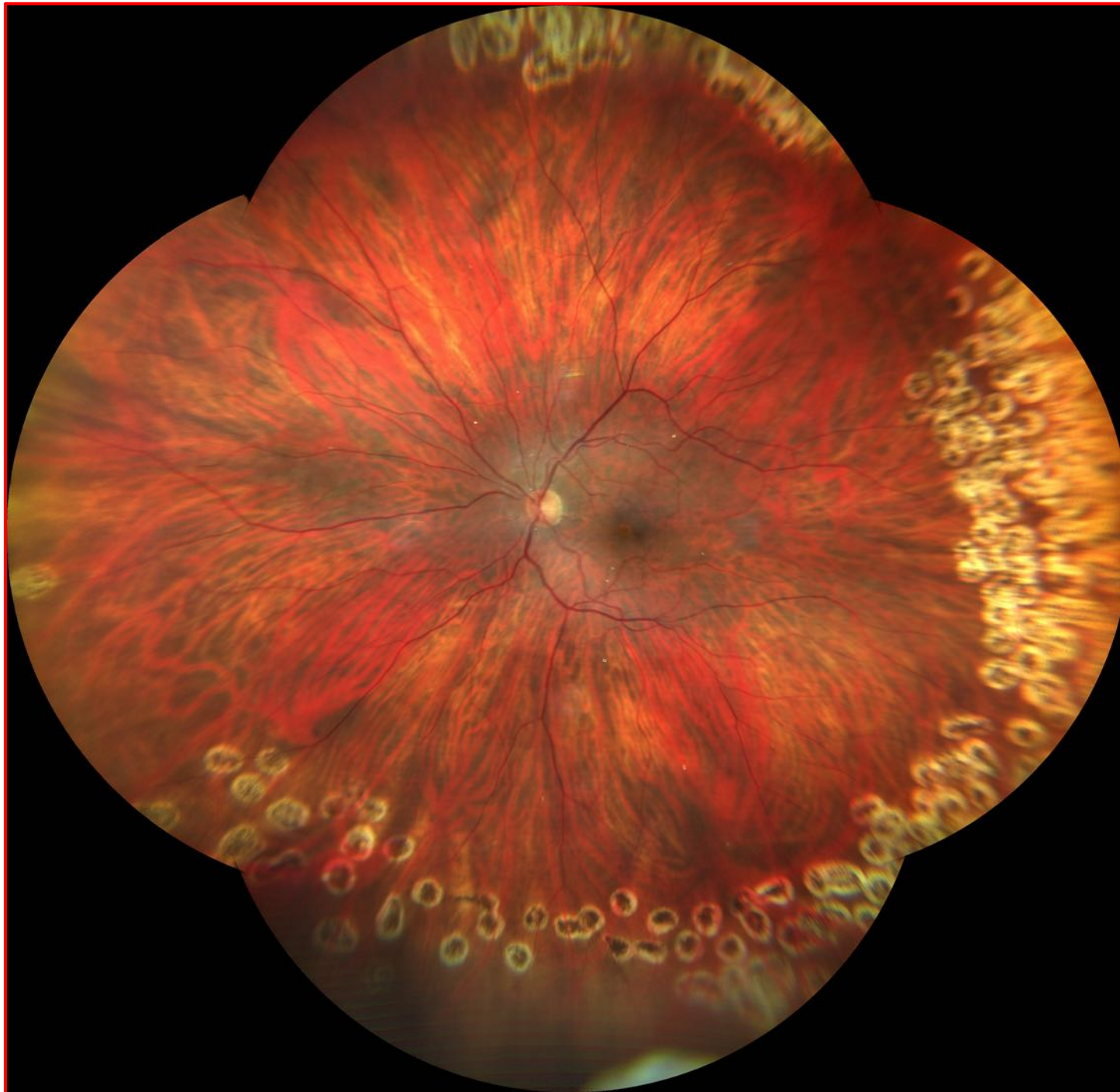
**Large chronic choroid detachment
after glaucoma surgery with MIGS
Minimally Invasive Glaucoma Surgery
MicroShunt PreserFlo (8,5 mm)
Tonometry 4/6 mmH
Visus 5/10; 31/05/21**



**Large chronic choroid detachment
after glaucoma surgery with MIGS
Minimally Invasive Glaucoma Surgery
MicroShunt PreserFlo (8,5 mm)
Tonometry 6/8 mmHg
Visus 5/10; 10/11/21**

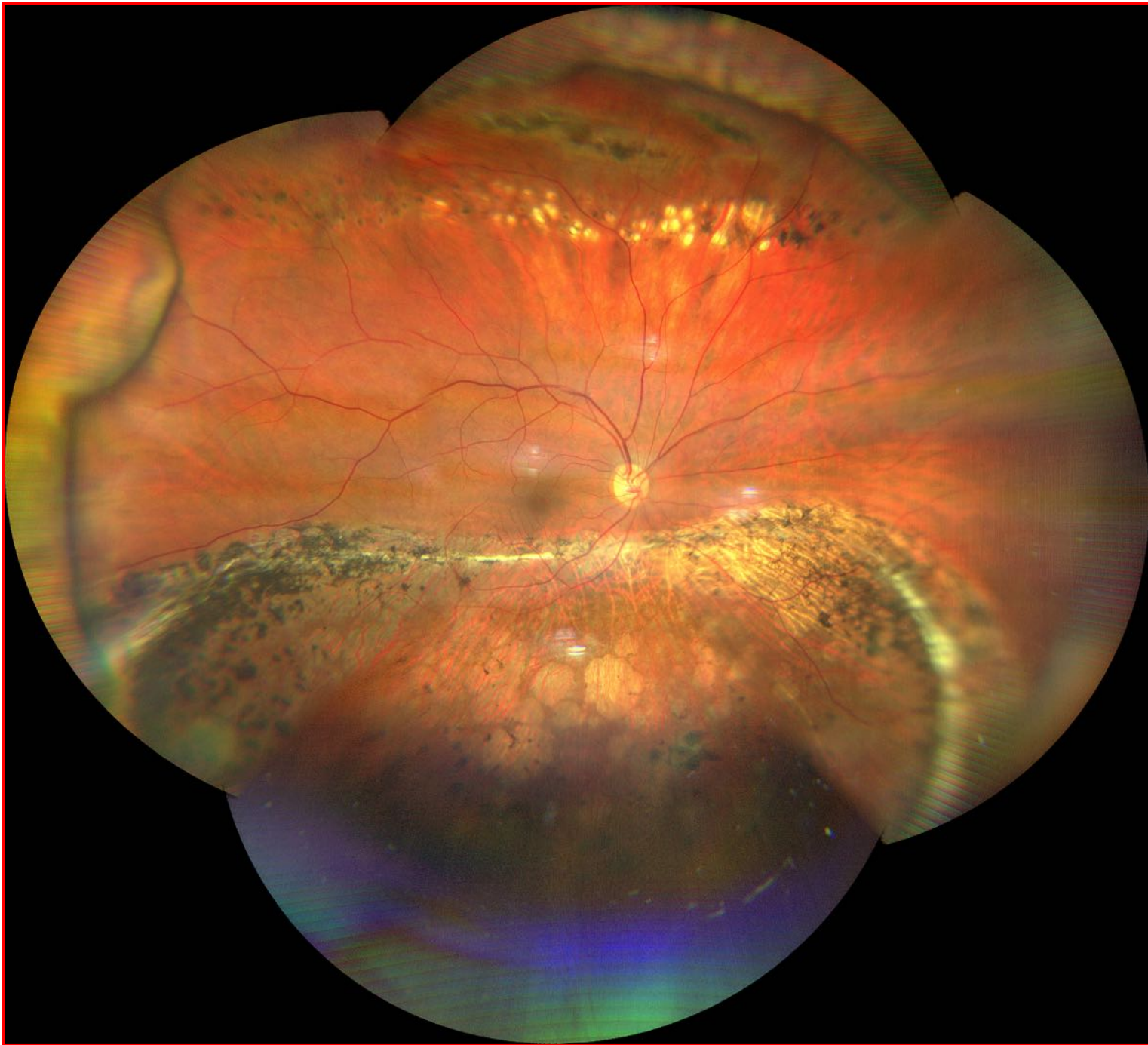
A fundus photograph of a retina, showing a large area of retinal detachment. The detached retina is visible as a pale, elevated, and wavy area on the right side of the image, contrasting with the normal reddish-orange color of the attached retina. The optic disc is visible on the left side, and the retinal vasculature is clearly seen throughout the field.

**Rapidly
evolving
monocular
retinal
detachment
in a young
woman
14/09/2020**

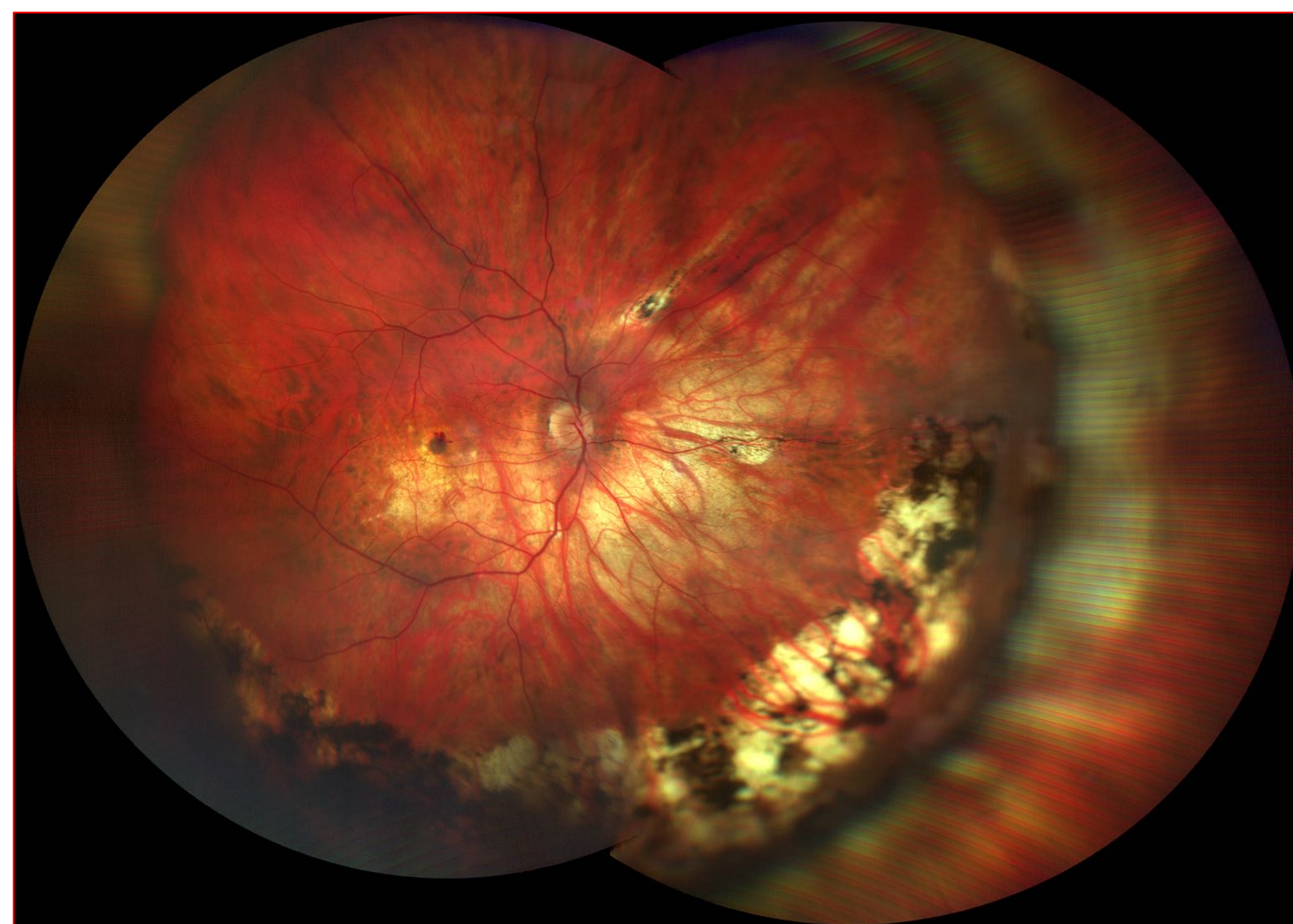


After treatment
rapidly
evolving
monocular
retinal
detachment
in a young
woman

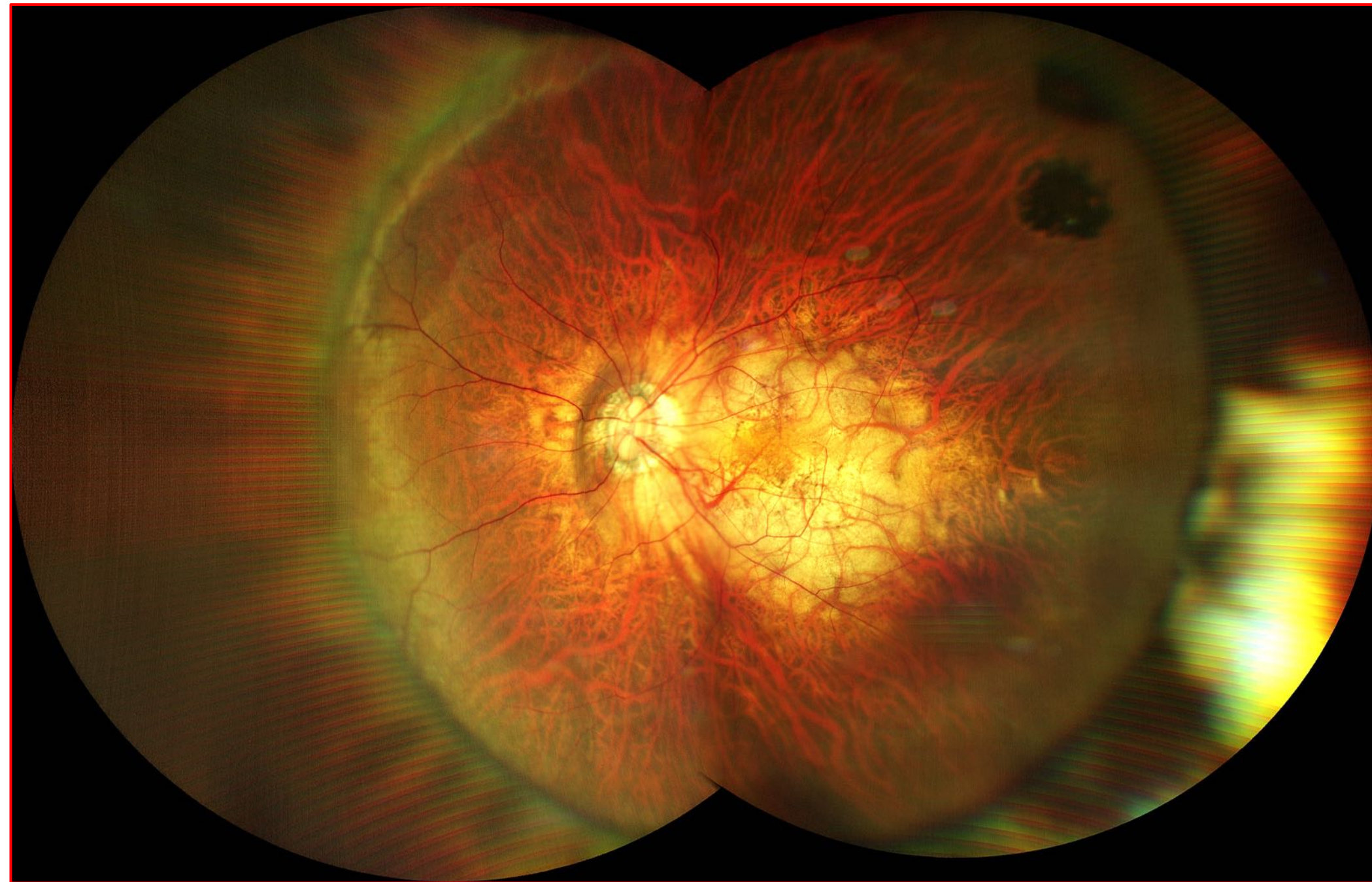




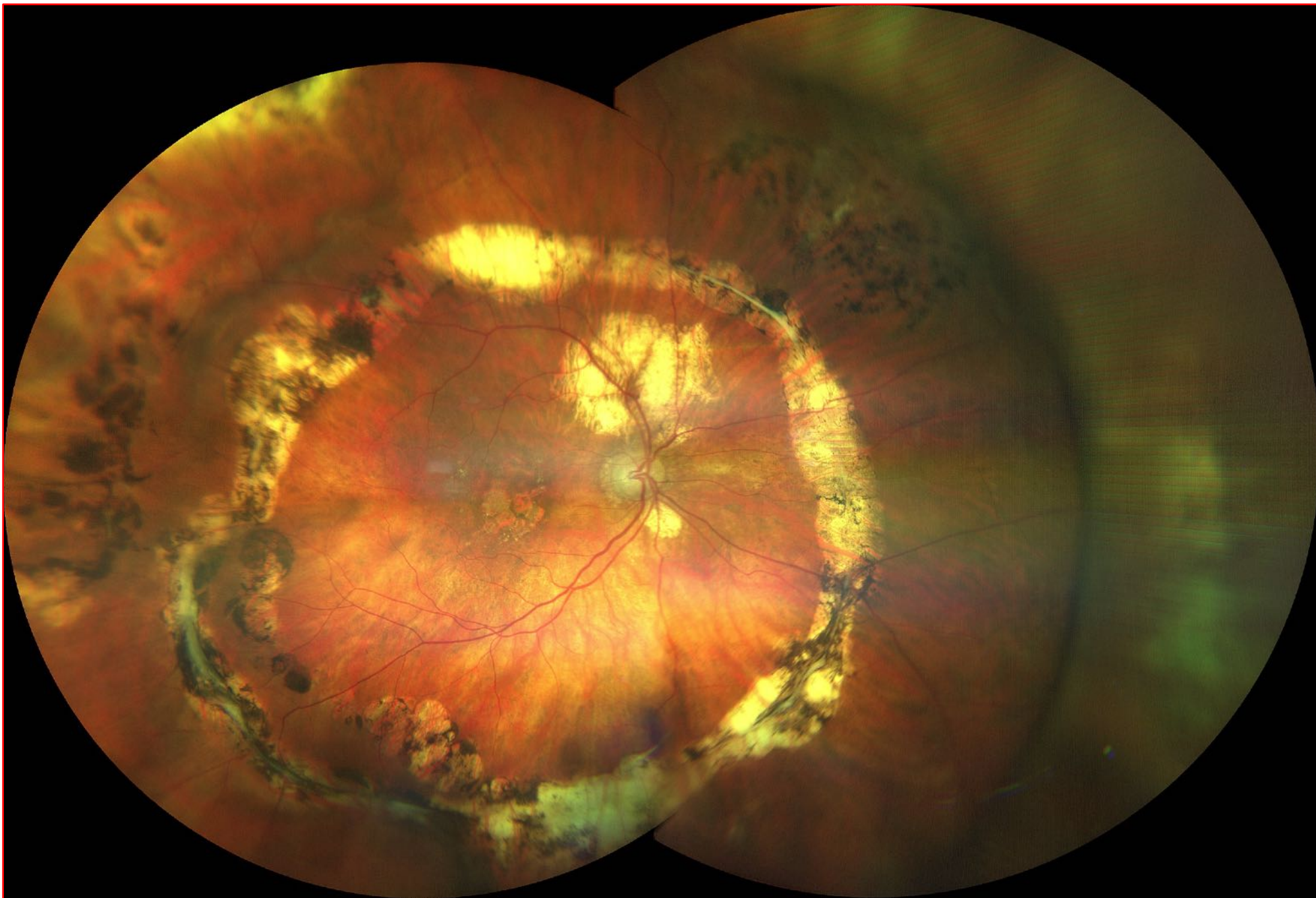
**Rhegmatogenous
retinal detachment with
retinal pigmentation**



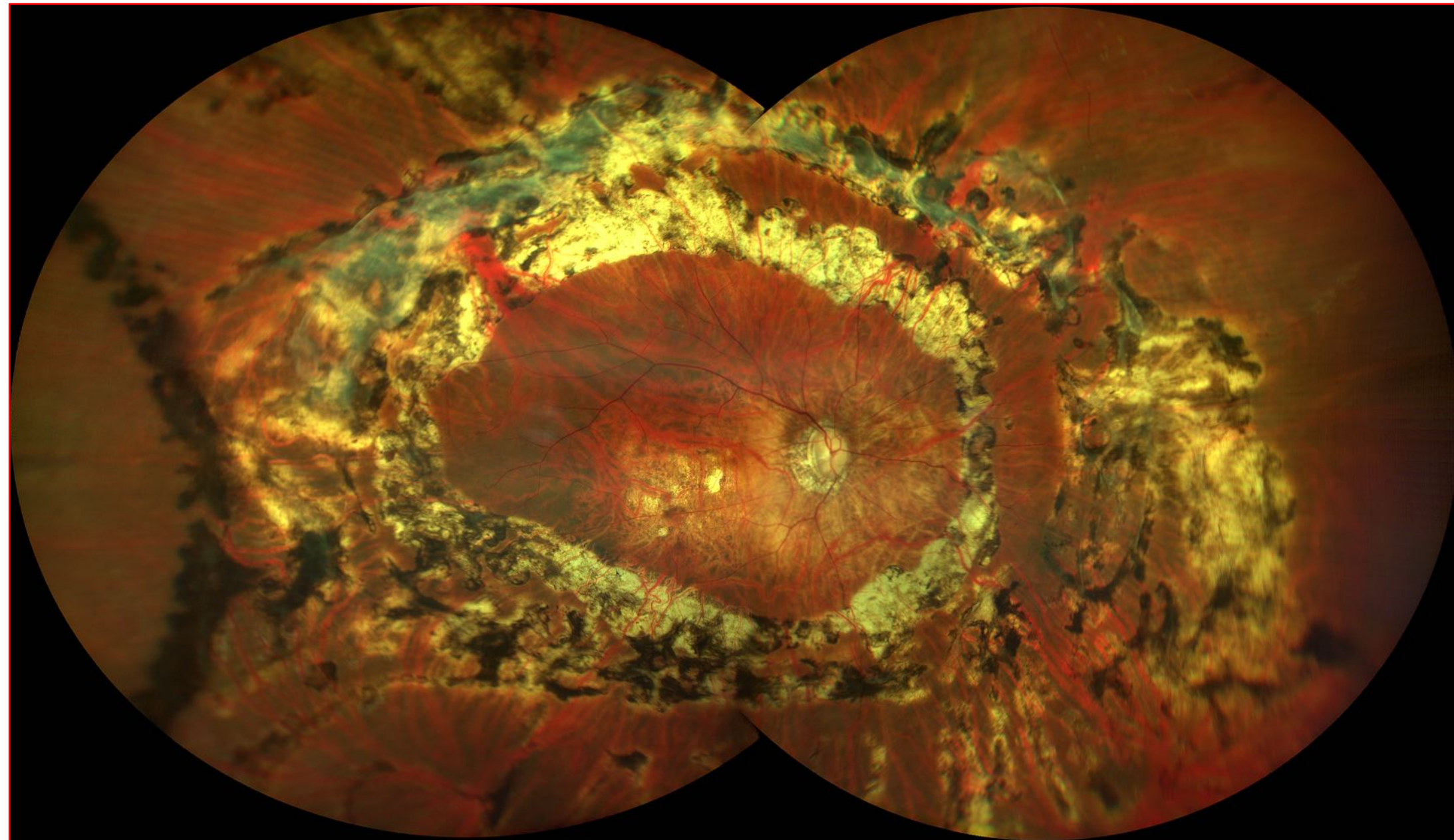
**Eyeball cerclage
for rhegmatogenous
retinal detachment
and cryotreatments
with macular CNV**



**Cerclage for
rhegmatogenous
retinal
detachment
in high
myopic eye with
large are of
atrophy**

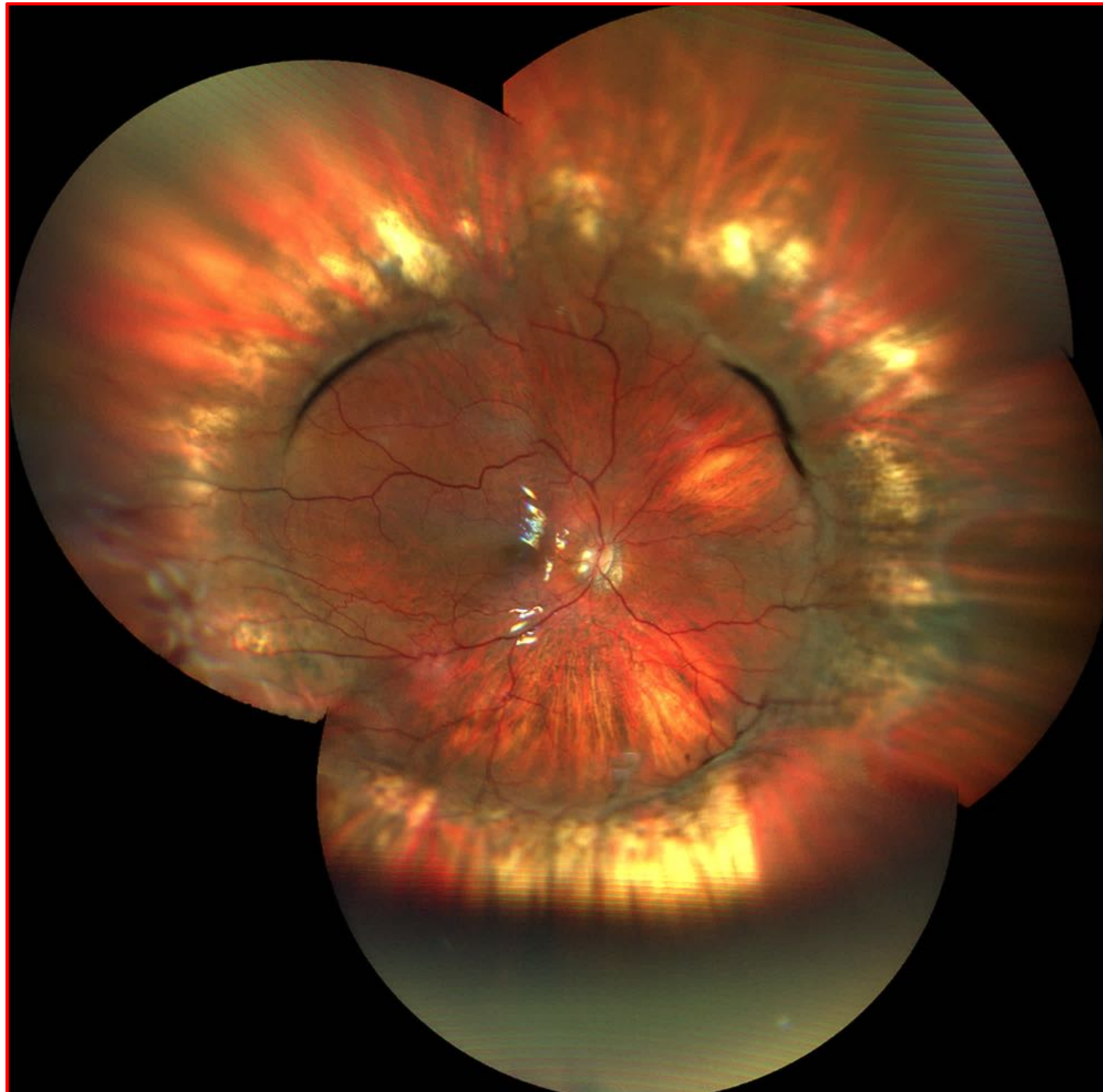


**Cerclage for
rhegmatogenous
retinal
detachment**

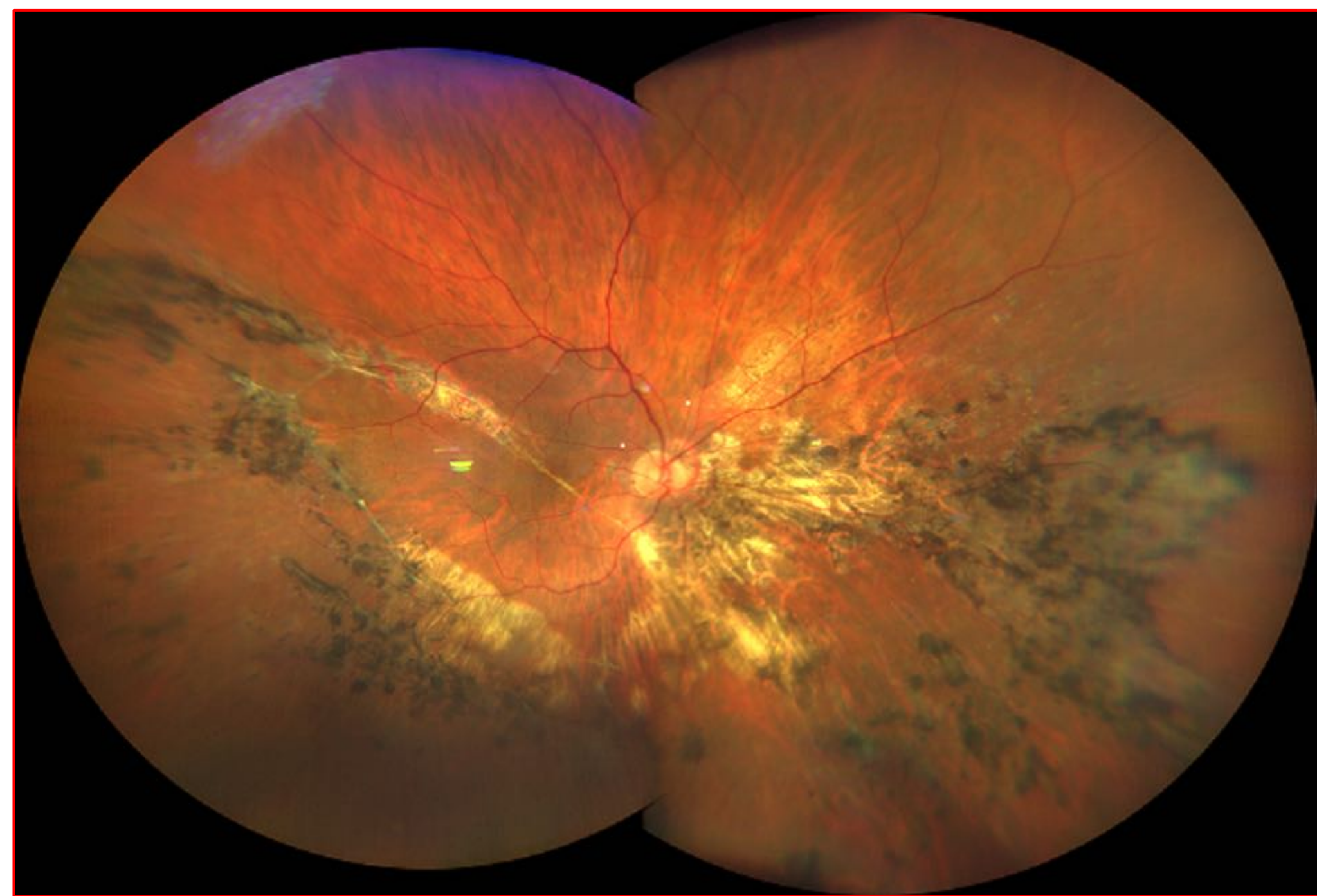


Retinal detachment with argon laser treatment

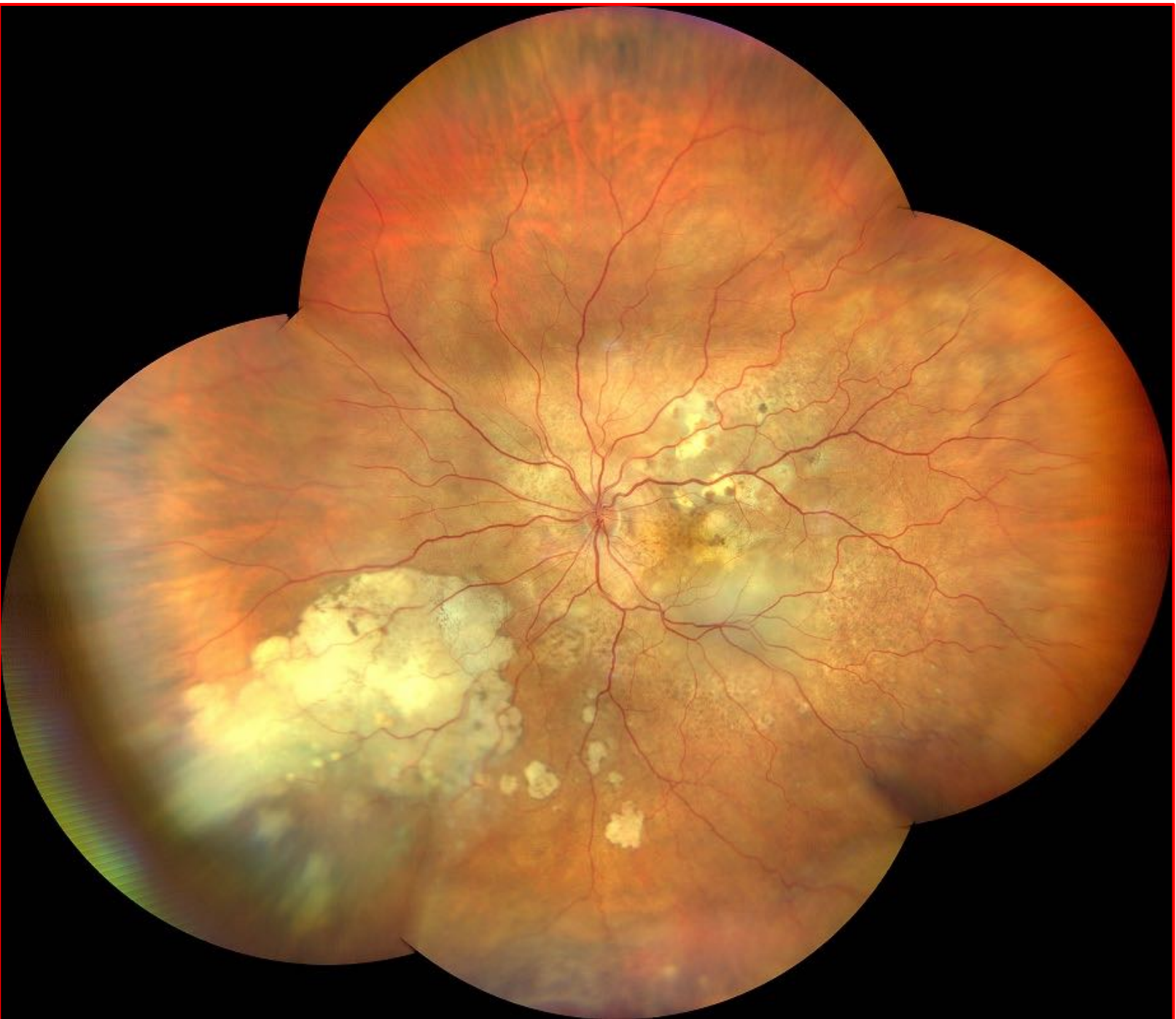




**Eyeball cerclage for
rhegmatogenous
retinal detachment**



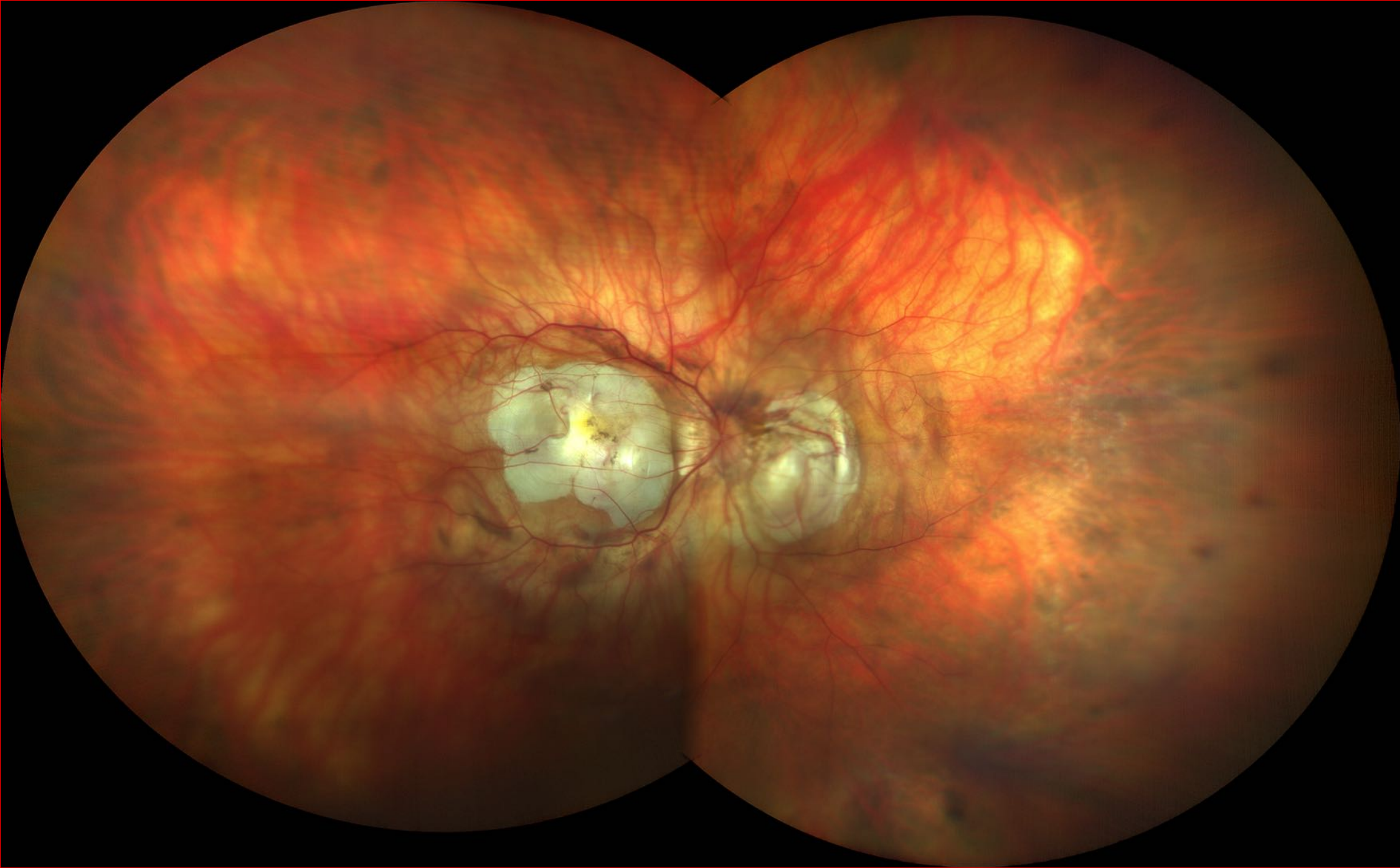
**Extensive
post-trauma
retinal
pigmentation
Visus 5/10**



Dramatic retinal picture in oncological patient with positive Batonella test fallowed elsewhere; Visus 1/20

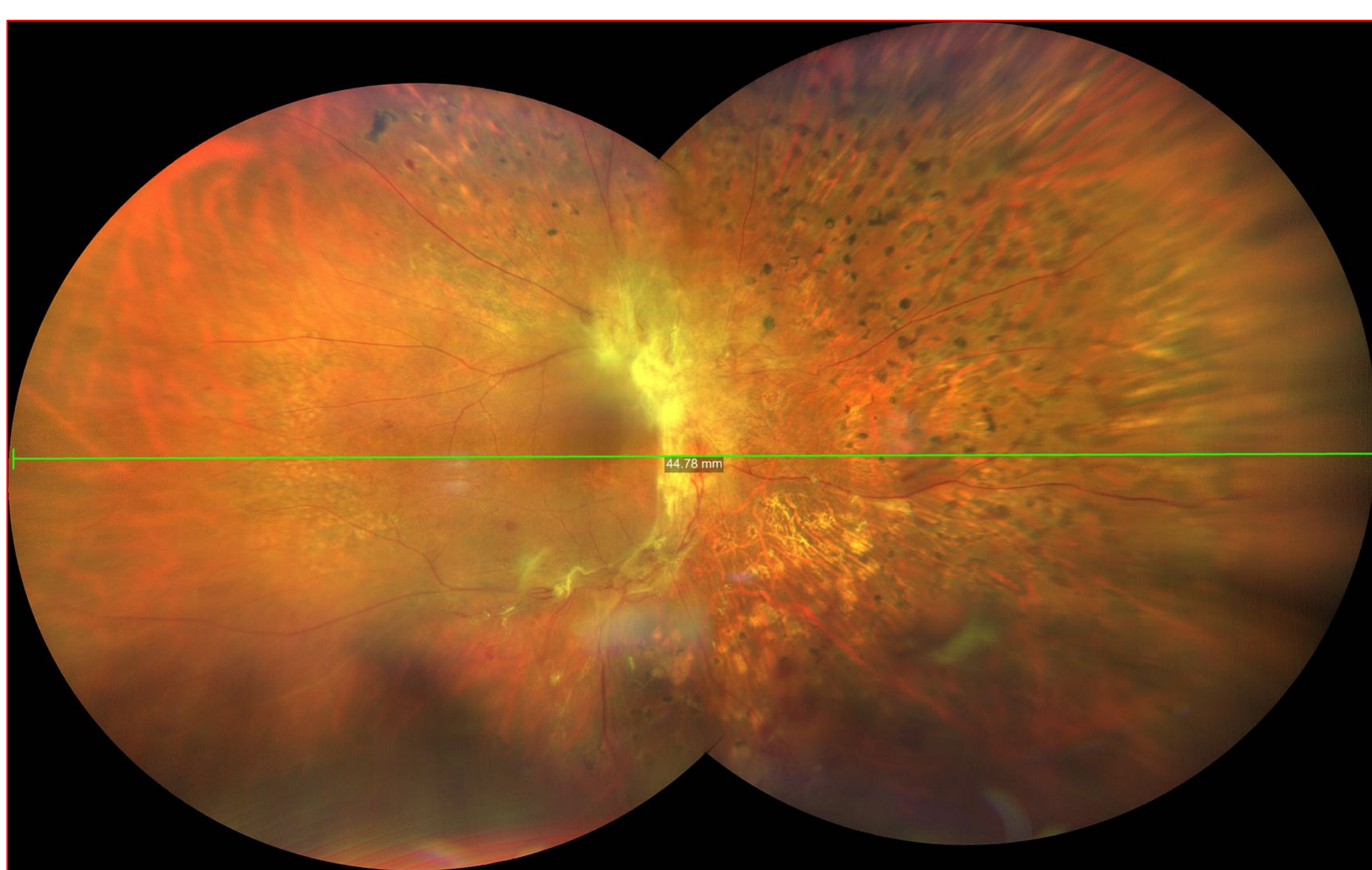


**Unnecessary
argon laser
treatment**



**High
myopia**

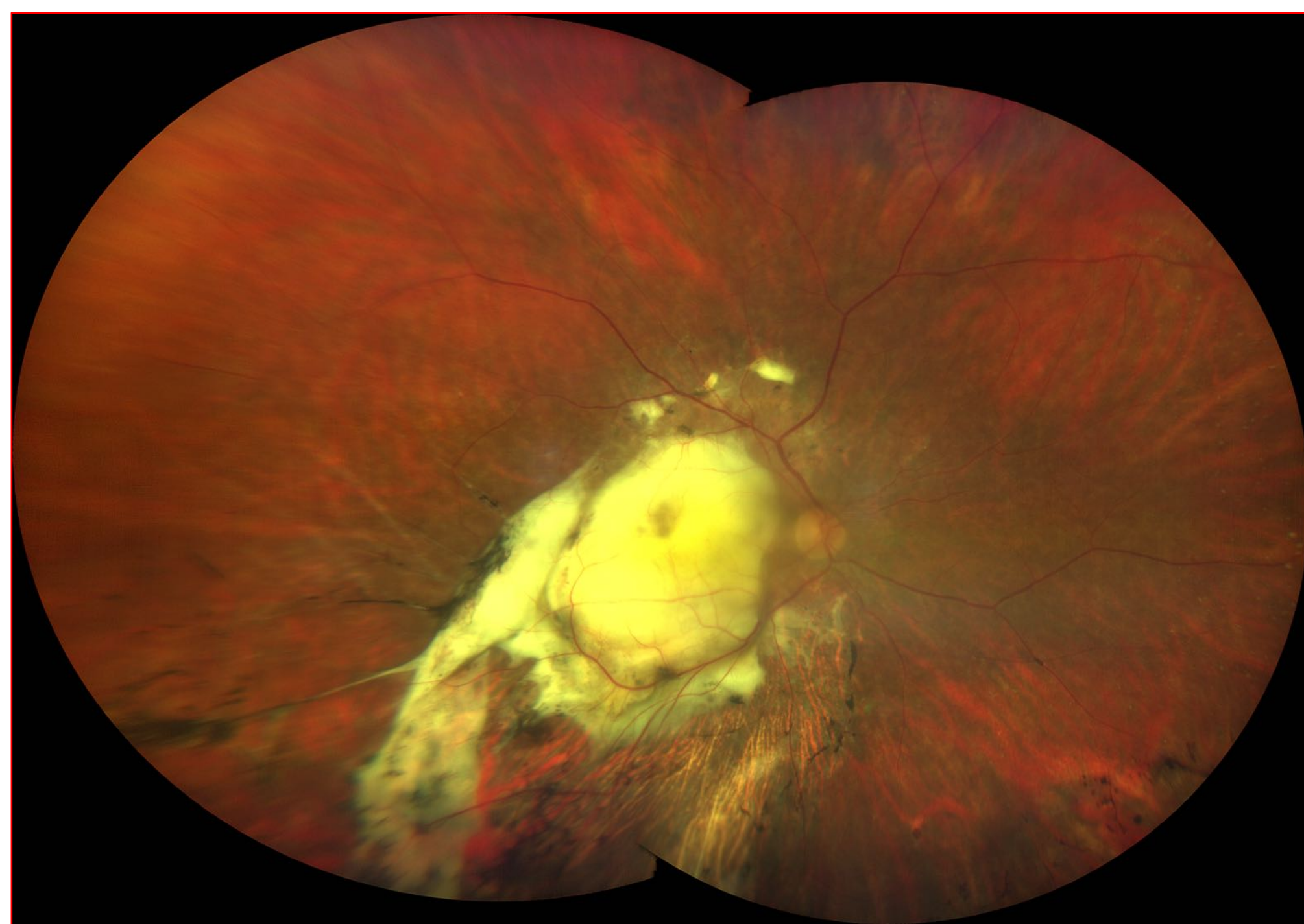




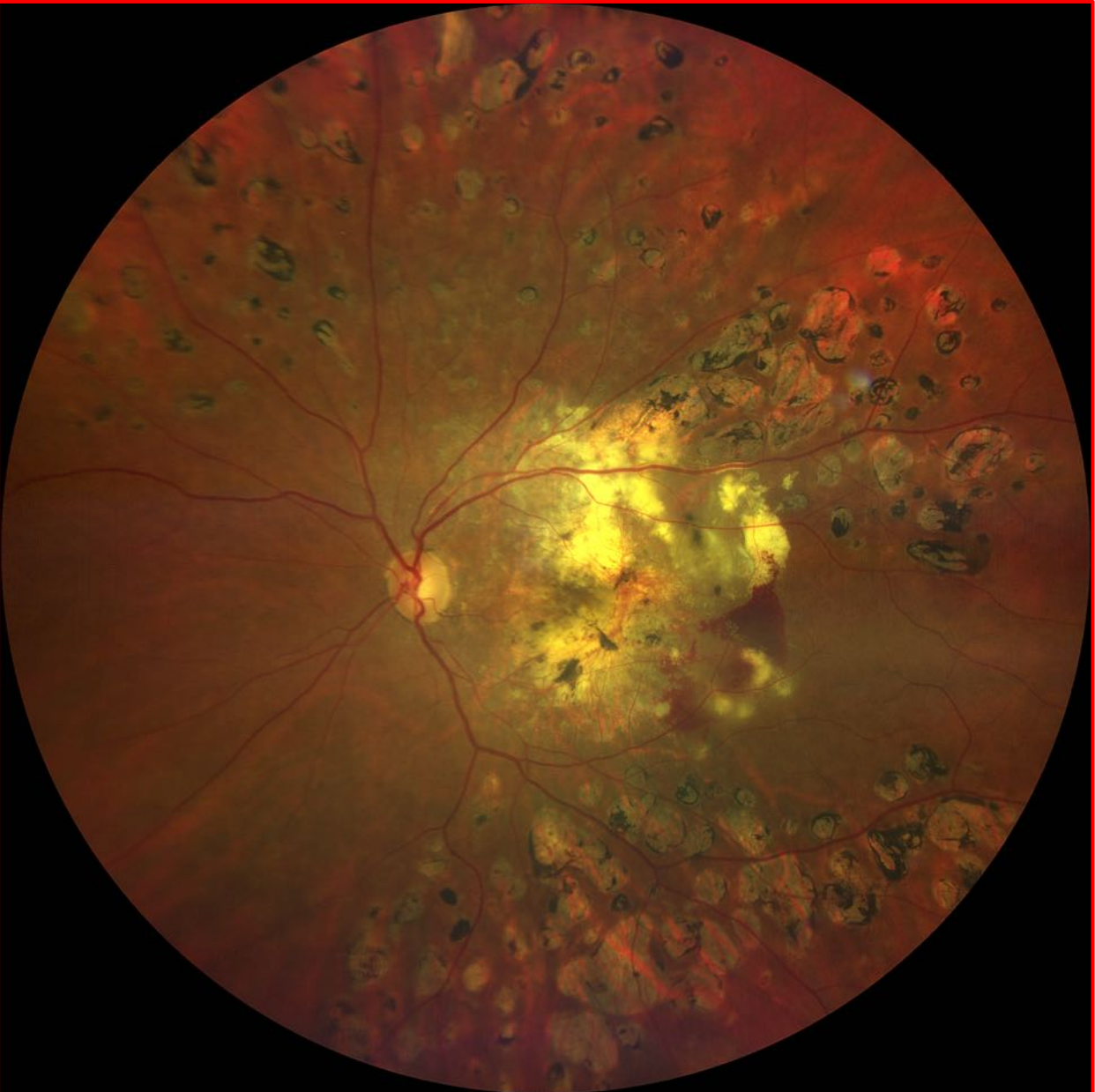
PDR
Proliferative
Diabetic
Retinopathy



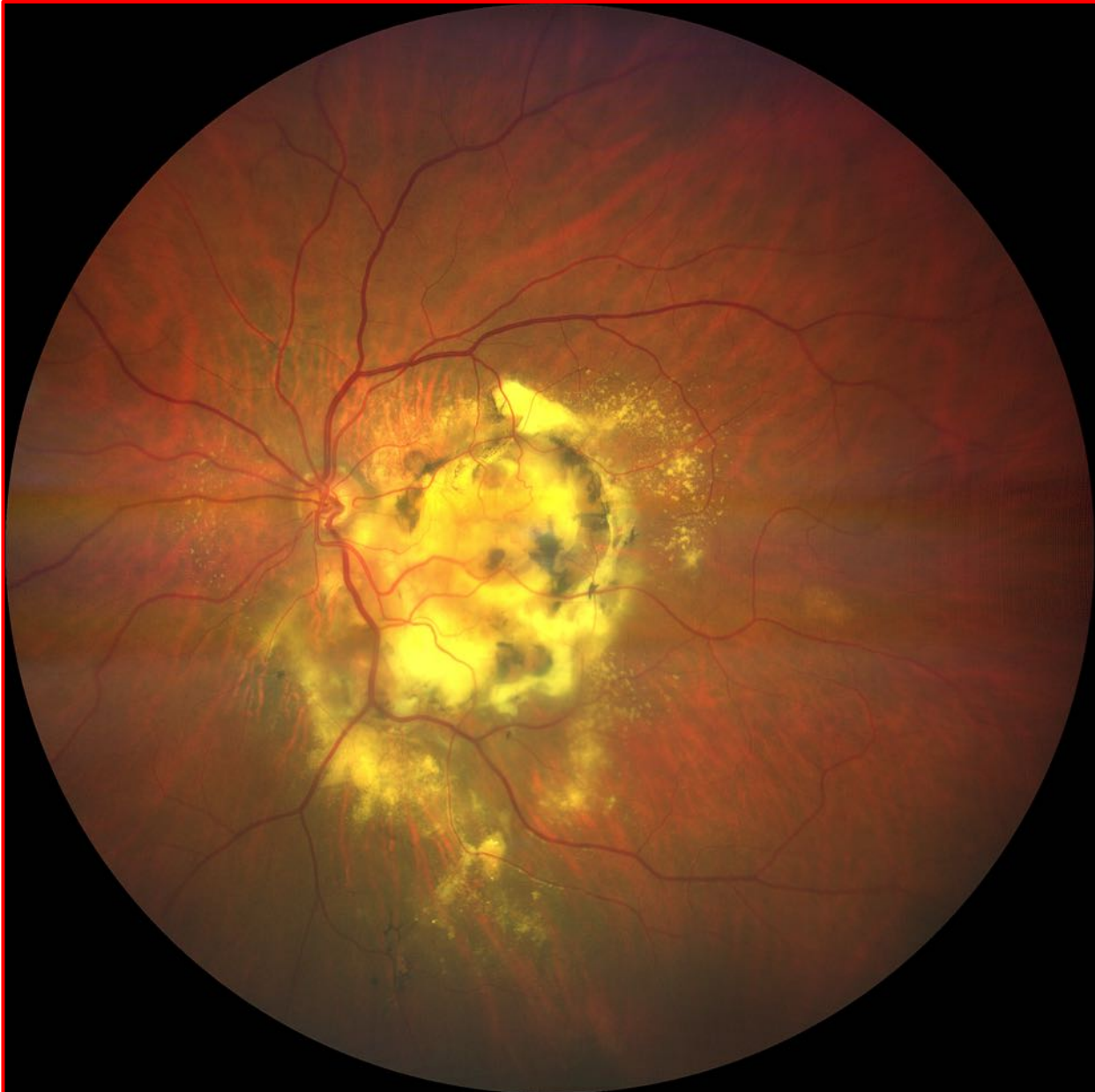
Retinopatia
Pigmentosa



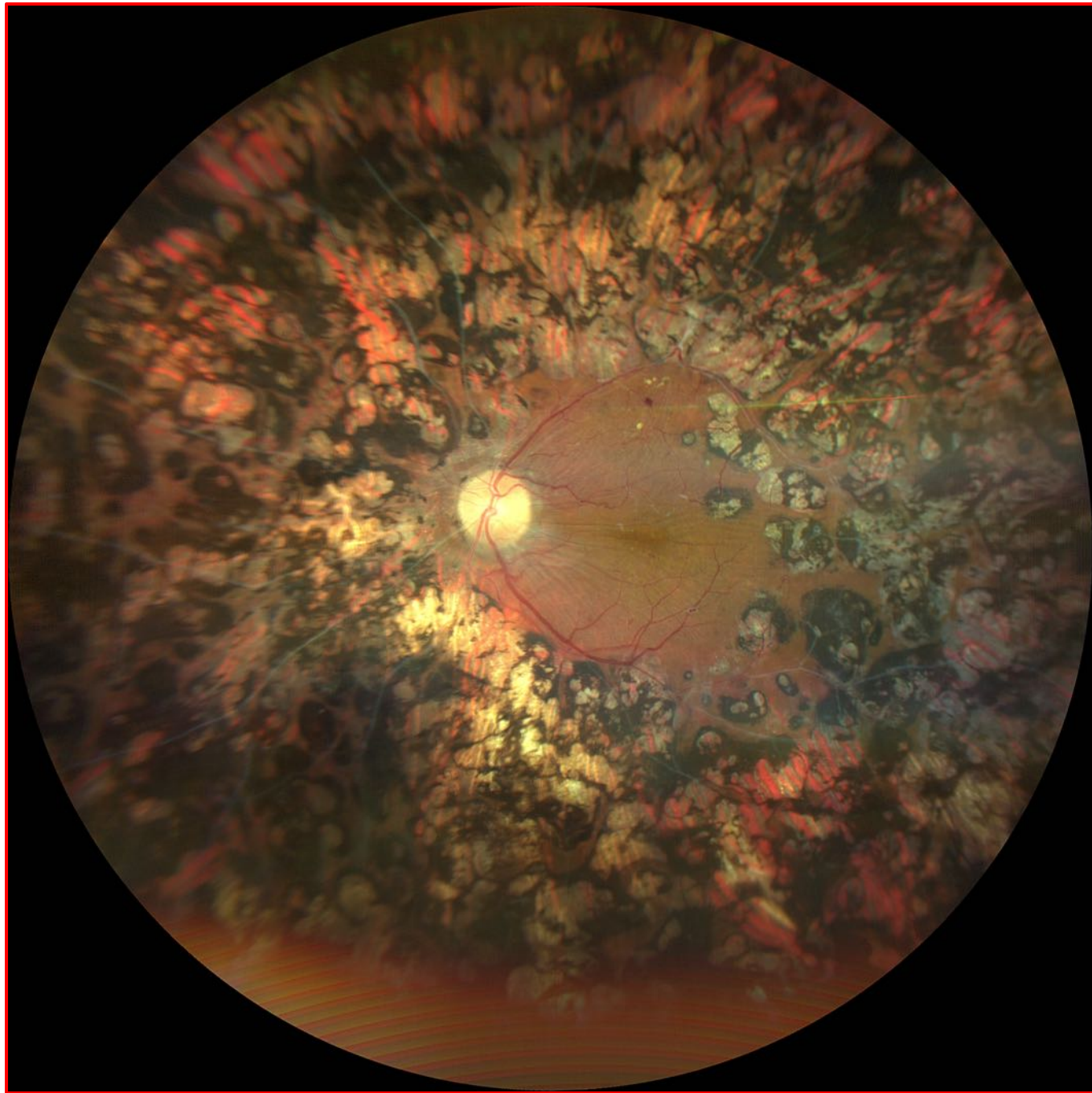
Advanced CNV



evolving CNV



advanced CNV

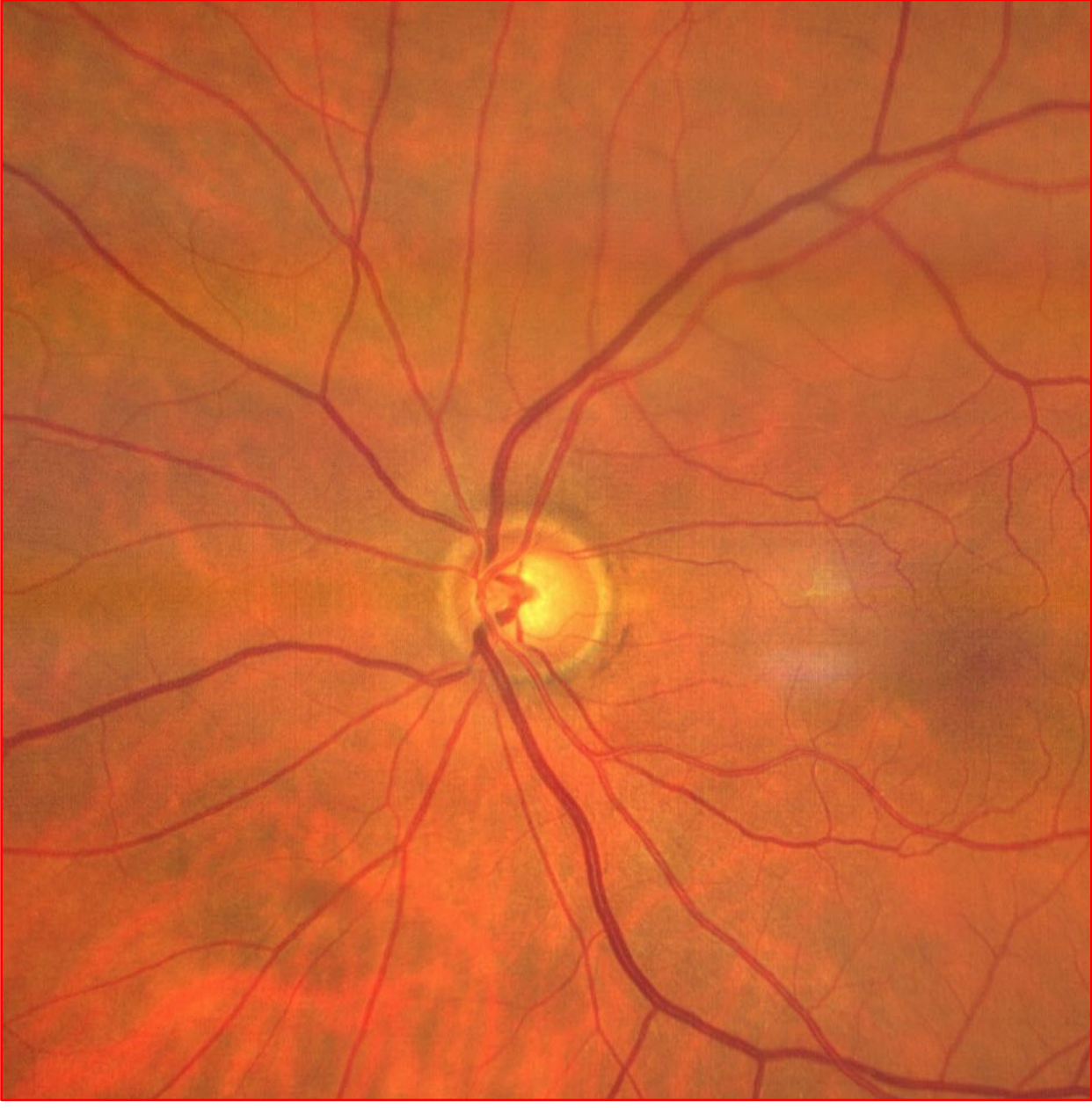
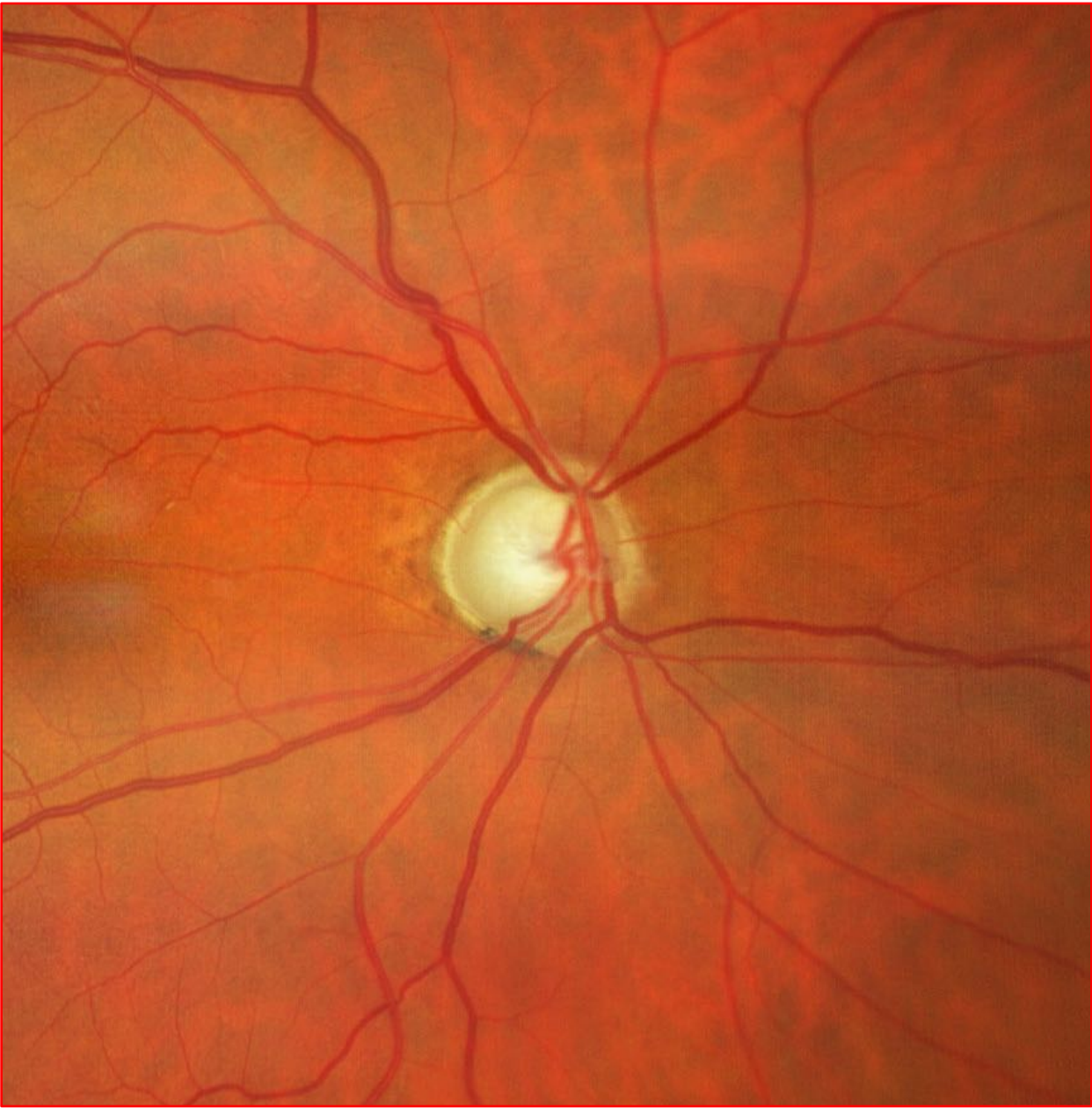


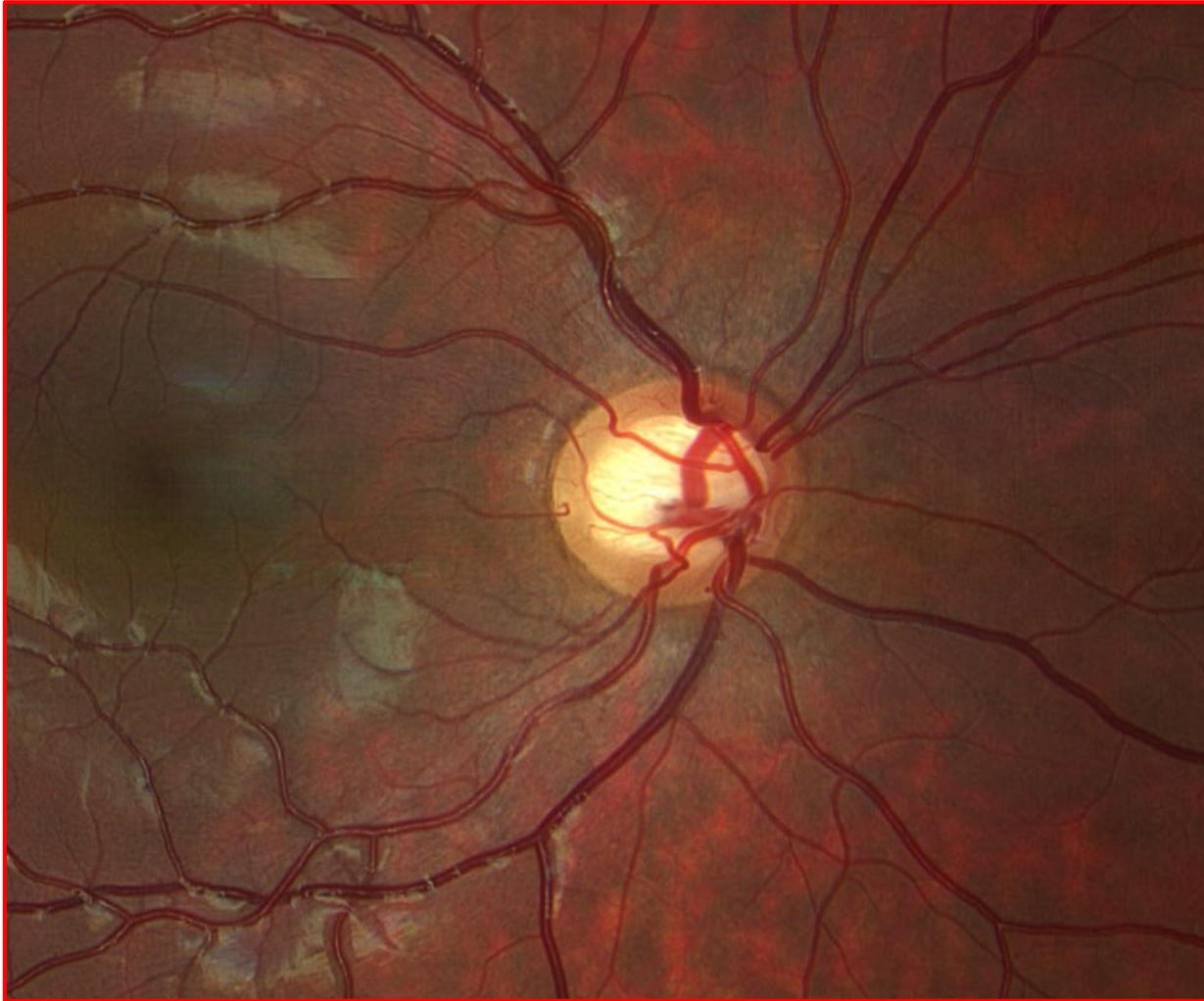
RD argon laser



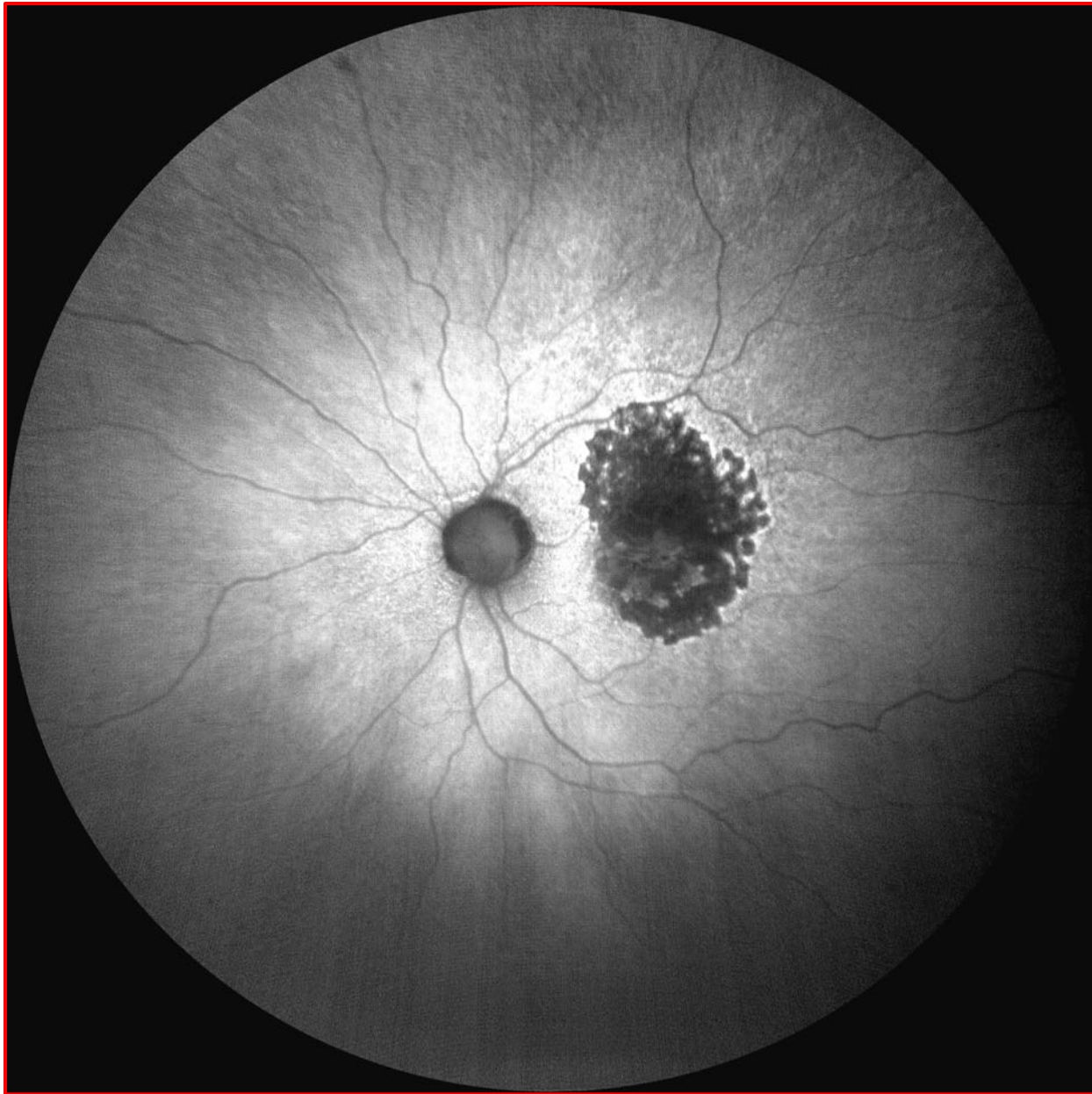


**Albinism with
nystagmus aa 9**

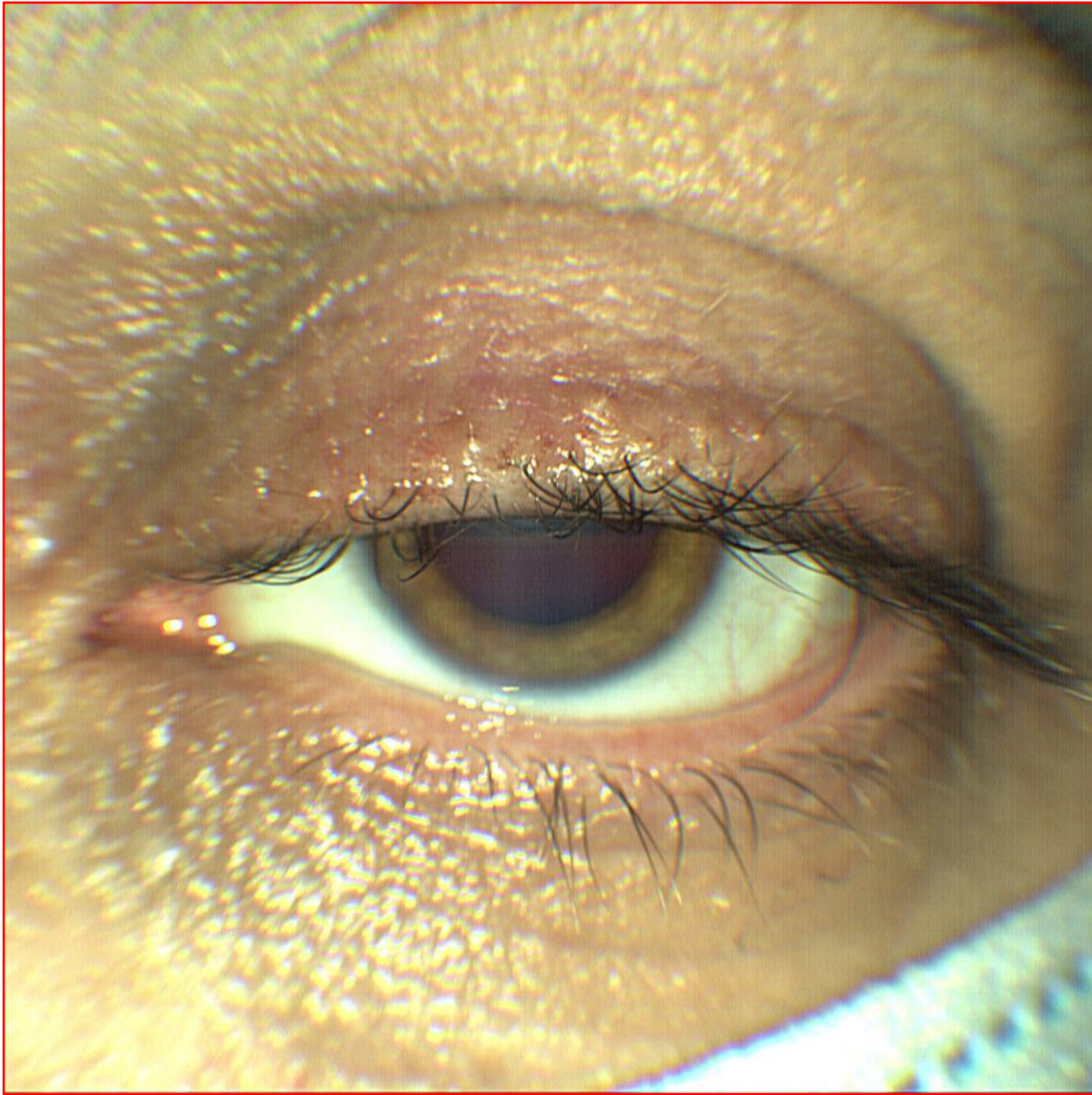
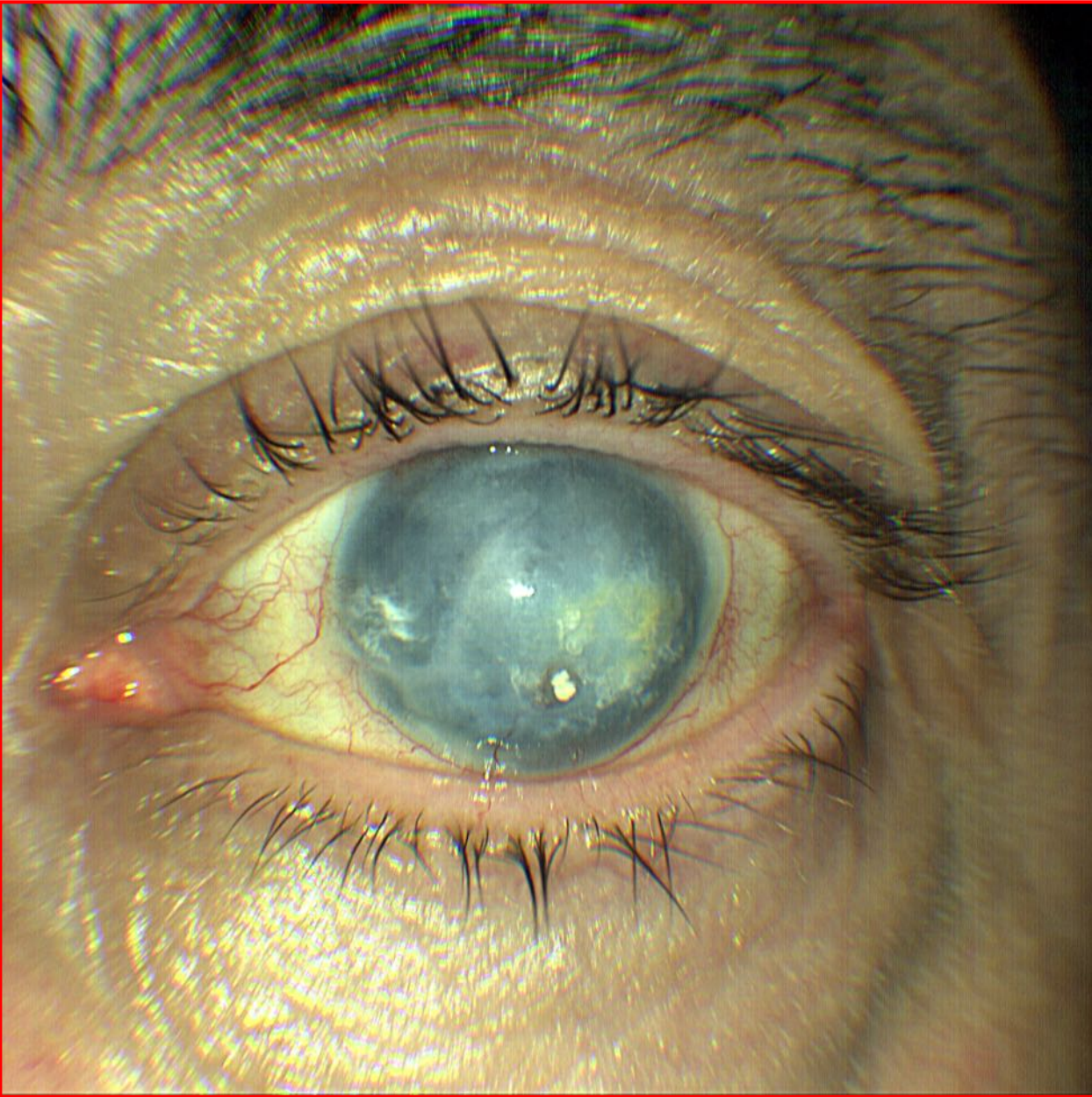




Bimbo di 8 anni paki 570 tono 16 mmHg





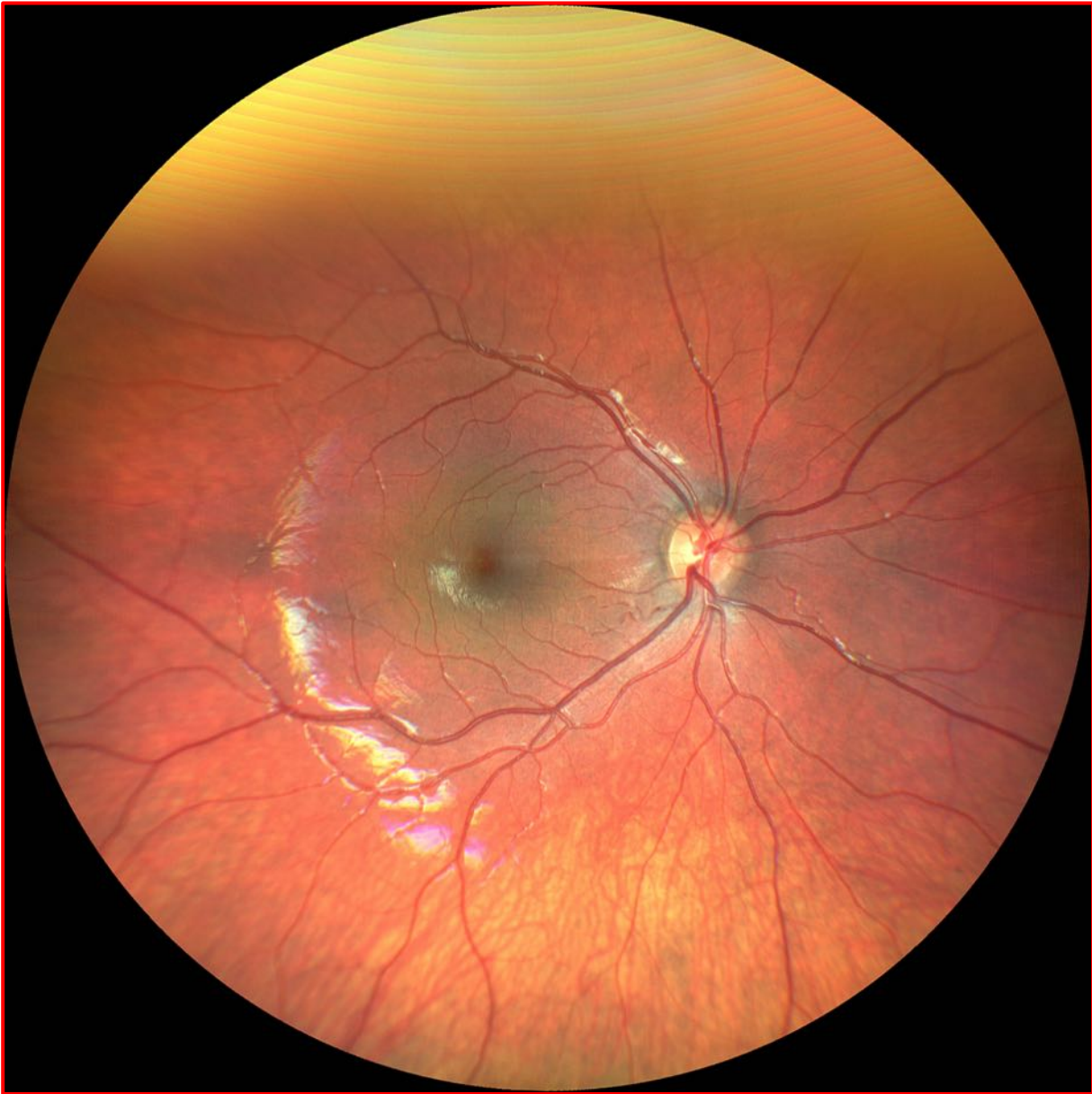


Widefield imaging a child of just 12 months

1 ammiccamento
0,3-0,4 sec

- Automatic Operations:**
- Autofocus automontage
 - Auto-exposure auto-laterality

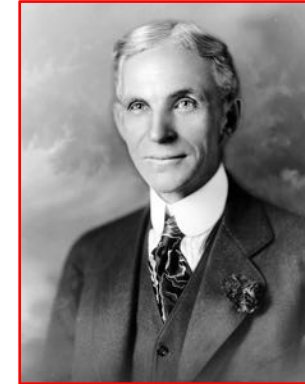
- Aquisition Speed:**
- Live IR Preview 10 frames/second
 - Image Capture 0.15 seconds



Basic References

- Wessel et al. affermano che l'utilizzo dell'UWFA aumenta del 10% l'area retinica interessata da alterazioni vasali nella **retinopatia diabetica**, non evidenziabile con FA. Br J Ophthalmol 2012;96:694-8
- Gupta V et al. suggeriscono che l'utilizzo di UWFA può allargare la possibilità di diagnosi nelle **uveiti posteriori** rispetto alla FA. Saudi J Ophthalmol 2014;28:95-103
- Leder HA et al. hanno studiato e dimostrato l'utilità del UWF nelle **vasculiti** non infettive e nella **Behçet**. J Ophthalmic Inflamm Infect 2013;3:30
- Prasad et al. riferiscono che il UWF è essenziale per una migliore diagnosi, gestione e trattamento delle **patologie vascolari**. Ophthalmology 2010;117:780-4
- Madhusudhan S. et al. hanno confermato l'importanza dell'ipossia e **dell'ischemia tissutale** della retina periferica come fattori patogenetici della **AMD e di NV**. The Scientific World Journal Vol 2014, Article ID 536161,7 pages
- Patel CK et al. affermano che le **Skip areas nella ROP** possono essere più agevolmente evidenziate con UWFA e trattate con laser e/o anti VEGF. Eye (Lond) 2013;27:589-96.
- Reznicek L et al. precisano che UWF facilita la diagnosi differenziale tra **melanoma maligno e nevo benigno** della coroide. Int J Ophthalmol 2014;7:697-703
- Le performances dell'UWF hanno trovato positiva applicazione inoltre nella **malattia di Coats** (Kang KB et al.), di **Von Hippel-Lindau** (Haddad NM et al.) e nel **distacco di retina**.
- A. Lucente. Evoluzione della fotografia retinica e Imaging Widefield. Oftalmologia domani Anno IX - 2018

**“C'è vero progresso solo quando i vantaggi di una nuova tecnologia diventano per tutti”
Henry Ford (1863 – 1947)**



Capitale stimato in 199 miliardi di dollari, nona persona più ricca della storia

Tin Lizzie (lucertolina di latta), **Flivver** (macinino) o semplicemente **Ford T**, Ford Motor Company dal 1908 al 1927

Prima vettura prodotta in grande serie utilizzando la catena di montaggio



Thank you for your kind attention!



Centro di eccellenza Zeiss per la diagnostica

www.amedeolucente.it